

2

**NAVAL POSTGRADUATE SCHOOL**  
**Monterey, California**

**AD-A277 841**



**94-10356**



**DTIC**  
**ELECTE**  
**APR 06 1994**  
**S B D**

**THESIS**

**CYLINDER DRAG EXPERIMENT -**  
**AN**  
**UPGRADED LABORATORY**

by

**Clayton William Miller**

**December 1993**

**Thesis Advisor:**  
**Co-Advisor:**

**Richard M. Howard**  
**Joseph W. Sweeney III**

Approved for public release; distribution is unlimited.

DTIC QUALITY INSPECTED 3

**94 4 5 059**

REPORT DOCUMENTATION PAGE			Form Approved OMB No. 0704
Public reporting burden for this collection of information is estimated to average 1 hour per response, including the time for reviewing instruction, searching existing data sources, gathering and maintaining the data needed, and completing and reviewing the collection of information. Send comments regarding this burden estimate or any other aspect of this collection of information, including suggestions for reducing this burden, to Washington Headquarters Services, Directorate for Information Operations and Reports, 1215 Jefferson Davis Highway, Suite 1204, Arlington, VA 22202-4302, and to the Office of Management and Budget, Paperwork Reduction Project (0704-0188) Washington DC 20503.			
1. AGENCY USE ONLY (Leave blank)	2. REPORT DATE December 1993	3. REPORT TYPE AND DATES COVERED Master's Thesis	
4. TITLE AND SUBTITLE CYLINDER DRAG EXPERIMENT - AN UPGRADED LABORATORY		5. FUNDING NUMBERS	
6. AUTHOR(S) Miller, Clayton William			
7. PERFORMING ORGANIZATION NAME(S) AND ADDRESS(ES) Naval Postgraduate School Monterey CA 93943-5000		8. PERFORMING ORGANIZATION REPORT NUMBER	
9. SPONSORING/MONITORING AGENCY NAME(S) AND ADDRESS(ES)		10. SPONSORING/MONITORING AGENCY REPORT NUMBER	
11. SUPPLEMENTARY NOTES The views expressed in this thesis are those of the author and do not reflect the official policy or position of the Department of Defense or the U.S. Government.			
12a. DISTRIBUTION/AVAILABILITY STATEMENT Approved for public release; distribution is unlimited.		12b. DISTRIBUTION CODE AA/Ho	
13. ABSTRACT (maximum 200 words) A generalized automated data acquisition system was designed for the Naval Postgraduate School Aerolab Low Speed Wind Tunnel. A specific application of this system was to upgrade the current "Cylinder Drag Experiment" conducted during AA2801 "Aero Laboratories I", an introductory aeronautical laboratory course taught at the Naval Postgraduate School. Two methods of drag determination were used: pressure distribution and wake analysis (momentum method). Data from these two methods were collected by a system based on a high speed analog/digital computer board, a standard 486 IBM-type PC and data acquisition software. Characteristic methods of reducing data from this experiment are discussed. The results obtained by analyzing the acquired data compared favorably to empirical data from previous circular cylinder coefficient of drag experiments. This automated data acquisition system will facilitate future research and instructional use of the wind tunnel.			
14. SUBJECT TERMS Cylinder Drag Experiment, Automated Data Acquisition, Low Speed Wind Tunnel, Pressure Distribution Method, Wake Analysis Method (Momentum Method), LabTech Notebook Application, Student Wind Tunnel Laboratory Upgrade.			15. NUMBER OF PAGES 111
			16. PRICE CODE
17. SECURITY CLASSIFICATION OF REPORT Unclassified	18. SECURITY CLASSIFICATION OF THIS PAGE Unclassified	19. SECURITY CLASSIFICATION OF ABSTRACT Unclassified	20. LIMITATION OF ABSTRACT UL

NSN 7540-01-280-5500

Standard Form 298 (Rev. 2-89)

Prescribed by ANSI Std. Z39-18

DWC QUALITY CONTROLLED 3

Approved for public release; distribution is unlimited.

Cylinder Drag Experiment -

an

Upgraded Laboratory

by

Clayton W. Miller

Lieutenant Commander, United States Navy

B.S., United States Naval Academy, 1982

Submitted in partial fulfillment  
of the requirements for the degree of

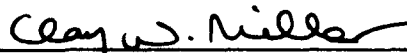
MASTER OF SCIENCE IN AERONAUTICAL ENGINEERING

from the

NAVAL POSTGRADUATE SCHOOL

December 1993

Author:

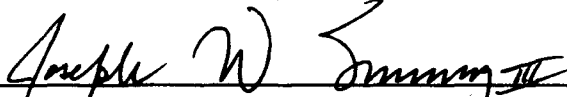


Clayton W. Miller

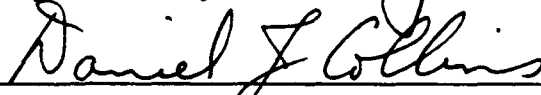
Approved by:



Richard M. Howard, Thesis Advisor



Joseph W. Sweeney III, Co-Advisor



Daniel J. Collins, Chairman

Department of Aeronautics & Astronautics

## ABSTRACT

A generalized automated data acquisition system was designed for the Naval Postgraduate School Low Speed Wind Tunnel. A specific application of this system was to upgrade the current "Cylinder Drag Experiment" conducted during AA2801 "Aero Laboratories I", an introductory aeronautical laboratory course taught at the Naval Postgraduate School. Two methods of drag determination were used: pressure distribution and wake analysis (momentum method). Data from these two methods were collected by a system based on a high speed analog/digital computer board, a standard 486 IBM-type PC and data acquisition software. Characteristic methods of reducing data from this experiment are discussed. The results obtained by analyzing the acquired data compared favorably to empirical data from previous circular cylinder coefficient of drag experiments. This automated data acquisition system will facilitate future research and instructional use of the wind tunnel.

Accession For	
NTIS GRA&I	<input checked="checked" type="checkbox"/>
DTIC TAB	<input type="checkbox"/>
Unannounced	<input type="checkbox"/>
Justification	
By	
Distribution/	
Availability Codes	
Dist	Avail and/or Special
A-1	

## TABLE OF CONTENTS

I. INTRODUCTION .....	1
II. N.P.S. LOW SPEED WIND TUNNEL .....	3
A. DESCRIPTION AND OPERATING PROCEDURES .....	3
B. CORRECTION FACTORS .....	7
C. CALIBRATION AND RESULTS .....	11
III. CYLINDER DRAG THEORY .....	18
A. AERODYNAMIC DRAG CLASSIFICATION .....	18
B. MEASURING DRAG BY PRESSURE DISTRIBUTION .....	19
C. MEASURING DRAG BY WAKE ANALYSIS (MOMENTUM) ...	25
IV. AA2801 CYLINDER LAB .....	29
A. PREVIOUS LABORATORY .....	29
B. UPGRADED LABORATORY .....	32
V. RESULTS .....	49
A. ACTUAL CLASS DATA (USING DRAG1.M) .....	49

B.	PRESSURE DISTRIBUTION METHOD (RUN #1) . . . . .	50
C.	WAKE ANALYSIS METHOD (RUNS #2,3) . . . . .	54
VI.	CONCLUSIONS . . . . .	58
A.	UPGRADE LIMITATIONS . . . . .	58
B.	RECOMMENDATIONS . . . . .	60
	APPENDIX A: PREVIOUS LAB HANDOUT . . . . .	63
	APPENDIX B: UPGRADED LAB HANDOUT . . . . .	68
	APPENDIX C: UPGRADED LAB DATA . . . . .	83
	APPENDIX D: MATLAB CODE FOR RETRIEVAL/DATA ANALYSIS . . . . .	92
	APPENDIX E: MATLAB CODES FOR TUNNEL VELOCITY TABLES . . . . .	94
	LIST OF REFERENCES . . . . .	97
	INITIAL DISTRIBUTION LIST . . . . .	98

## **LIST OF TABLES**

Table 1. Test Section Dimensions . . . . .	4
Table 2. Wind Tunnel Operating Procedures . . . . .	6
Table 3. Step Two Results . . . . .	14
Table 4. Drag Classification . . . . .	18
Table 5. Drag1.m Results . . . . .	51

## **APPENDIX B**

Table 1. Drag Classification . . . . .	69
Table 2. File Organization . . . . .	71
Table 3. AA2801 Cylinder Lab Initial Settings . . . . .	74

## **LIST OF FIGURES**

Figure 1. The Test Section Showing The Wake Traverse and Probes Apparatus .	2
Figure 2. NPS Low Speed Wind Tunnel . . . . .	4
Figure 3. Test Section View - Into the Freestream . . . . .	5
Figure 4. Test Section View - Looking Down Wind . . . . .	6
Figure 5. N.P.S. Low Speed Wind Tunnel Water Manometer . . . . .	8
Figure 6. The "Schmidter" (a calibration manometer) . . . . .	12
Figure 7. Data From Step One of the Calibration . . . . .	14
Figure 8. Calibration Curve from Step Two data . . . . .	16
Figure 9. Pressure Forces on the Surface of a Cylinder . . . . .	19



Figure 10. Inviscid $C_p$ as Compared to Actual $C_p$ . . . . .	24
Figure 11. $C_p \cdot \cos\theta$ compared to $C_p$ . . . . .	25
Figure 12. Hewlett & Packard X-Y Plotters. . . . .	30
Figure 13. Signal Path of Data Acquisition System . . . . .	32
Figure 14. 486DX/33 MHz PC Used For Data Acquisition . . . . .	33
Figure 15. Electrically Rotatable Base for Cylinder . . . . .	35
Figure 16. N.P.S. Signal Conditioner . . . . .	36
Figure 17. LabTech Notebook Set-Up "PRE_DIS1" . . . . .	39
Figure 18. Actual LabTech Notebook Readout of $C_p$ vs. $\theta$ from Run #1 . . . . .	40
Figure 19. LabTech Notebook Set-Up "WAKE_AN1/2" . . . . .	44
Figure 20. The Separation Point Estimated by SEPAZ . . . . .	52

Figure 21. $C_p * \cos\theta$ vs. $\theta$ Compared To Matlab's 5th Order "POLYFIT" . . . .	53
Figure 22. WAKE_AN1 Results (Run #2) . . . . .	54
Figure 23. WAKE_AN2 Results Compared (Run #3) . . . . .	55
Figure 24. Results Plotted Against Emperical Data . . . . .	56
Figure 25. Graph of the Equation $y=\sqrt{x}-x$ . . . . .	58

#### APPENDIX A

Figure 21. Aerodynamic Forces on a Cylinder . . . . .	64
Figure 22. Cylinder Drag Coefficient . . . . .	67

#### APPENDIX B

Figure 21. Signal Path of Data Acquisition System . . . . .	70
Figure 22. ZERO Showing Signal Somewhere Less Than Zero Volts . . . . .	77
Figure 23. ZERO Showing Signal After Being "Flown" Up to Zero Volts . . . . .	77
Figure 24. Cylinder Drag Coefficient . . . . .	82

## TABLE OF SYMBOLS AND ABBREVIATIONS

$p_0$	= total (stagnation) pressure
$p$	= static pressure
$q$	= dynamic pressure = $p_0 - p$
$\rho_\infty$	= freestream density
$(p_0)_\infty$	= freestream total pressure (associated with freestream velocity)
$p_\infty$	= freestream static pressure (associated with freestream velocity)
$q_\infty$	= freestream dynamic pressure = $(p_0)_\infty - p_\infty$
$(p_0)_w$	= wake total pressure measured behind the cylinder at the probe ( $(p_0)_w$ assumed to = $(p_0)_\infty$ when taken outside wake)
$p_w$	= static pressure measured behind the cylinder at the probe ( $p_w$ assumed to = $p_\infty$ when taken outside wake)
$q_w$	= wake dynamic pressure = $(p_0)_w - p_w$
$p_{cyl}$	= pressure measured at the port on the cylinder
$C_p$	= pressure coefficient
$C_D$	= drag coefficient (3-D)
$c_d$	= drag coefficient relating to total drag or profile drag
$c_{dp}$	= drag coefficient relating to form drag only
$c_{du}$	= uncorrected drag coefficient
$\theta$	= azimuth of the rotator (signal from potentiometer)
$y$	= position of the traverse (signal from potentiometer)
$r$	= radius of cylinder
$R$	= gas constant
$d$	= diameter of the cylinder = $2 \times R$
$da$	= incremental area
$df$	= incremental pressure drag force
$dd$	= incremental form drag component
$dl$	= incremental induced drag component
$d$	= drag (2-D)
$l$	= length
$w$	= width
$h$	= height
$C$	= cross-sectional area
$F$	= measured force
$c$	= reference chord
$S$	= reference area
$A$	= area (2-D)
$V$	= volume (3-D)
$\epsilon$	= blockage factor
$V_\infty$	= freestream velocity
$V_w$	= velocity as measured along the traverse behind the cylinder

$V_{\text{into}}$  = the velocity into a closed system  
 $V_{\text{out}}$  = the velocity out of a closed system  
 $D$  = total drag unless specifically defined as "profile drag"  
 $D_f$  = shear drag - drag due to skin friction  
 $D_p$  = form drag - drag due to separation  
 $Re$  = Reynolds number  
 $e_{\text{ff}}$  = (subscript) effective (corrected value)  
 $u$  = (subscript) uncorrected value

## Conversion Constants

latitude correction = -0.0245 inches Hg  
 temperature correction (see Table 4-2 on bulletin board near tunnel)  
 $\mu_{\text{air}} = 3.8 \times 10^{-7} \text{ (lbf-s)/ft}^2$   
 $R_{\text{air}} = 53.3 \text{ (ft-lbf)/(lbm-}^\circ\text{R)}$   
 $^\circ\text{R} = ^\circ\text{F} + 460$   
 $1 \text{ ft} = 30.48 \text{ cm}$   
 $1 \text{ cm H}_2\text{O} = 0.0142 \text{ psi}$   
 $1 \text{ psi} = 2.036 \text{ inches Hg}$   
 $q_{\text{test section}} = (\Delta p - 0.243)/.895 \text{ (NPS wind tunnel calibration equation)}$   
 $TF = 1.04 \text{ (NPS wind tunnel turbulence factor)}$   
 $g_c = 32.174 \text{ ft/sec}^2 \text{ (universal gravitational constant)}$

## **ACKNOWLEDGEMENTS**

**"I called out of my distress to the LORD, and He answered me."**

**-Jonah, son of Amitta, from the stomach of the fish**

While I admit that I pestered every faculty member and student of the Aero Department at least once, this thesis and subsequent lab upgrade are gratefully dedicated to the motivation and patience offered by Professor Richard M. Howard and LCDR Joe Sweeney, to the technical assistance rendered daily to me by Jack King and to the ambition of my fellow classmates who are now still striving for academic excellence.

Most of all though, I dedicate this work to my beautiful wife Beverly, who with my four boys - Timothy, Benjamin, Seth and Nathaniel, did faithfully lift me up in prayer on a daily basis and sought God's help for a struggling engineer in the making.

## **I. INTRODUCTION**

A classic experiment, drag measurement over a circular cylinder in a wind tunnel, serves as an excellent primer on wind tunnel use, data acquisition and basic aerodynamics. This thesis served to upgrade an existing AA2801 (Aero Laboratories I) experimental lab (see Figure 1) while further exploring the theory behind the methods used to measure drag. Chapter II examines the Naval Postgraduate School's Low Speed Wind Tunnel, including a detailed procedure for calibrating the wind tunnel. Chapter III will discuss the theory behind drag measurements around a circular cylinder. Chapter IV compares the former and new procedures used in the AA2801 laboratory. The results of the new experiment using actual class data are then analyzed in Chapter V and some conclusions are drawn in Chapter VI. Appendix A contains the former AA2801 Cylinder Drag Experiment Handout. Appendix B contains a copy of the upgraded handout that was used on 9 November 1993 with a class of graduate students. Appendix C contains a readout of the experimental data obtained. Appendix D is the MATLAB script file "DRAG1.m" used to analyze data from the upgraded lab. Appendix E has several MATLAB script files for creating velocity tables and curves which were derived from wind tunnel calibration data.

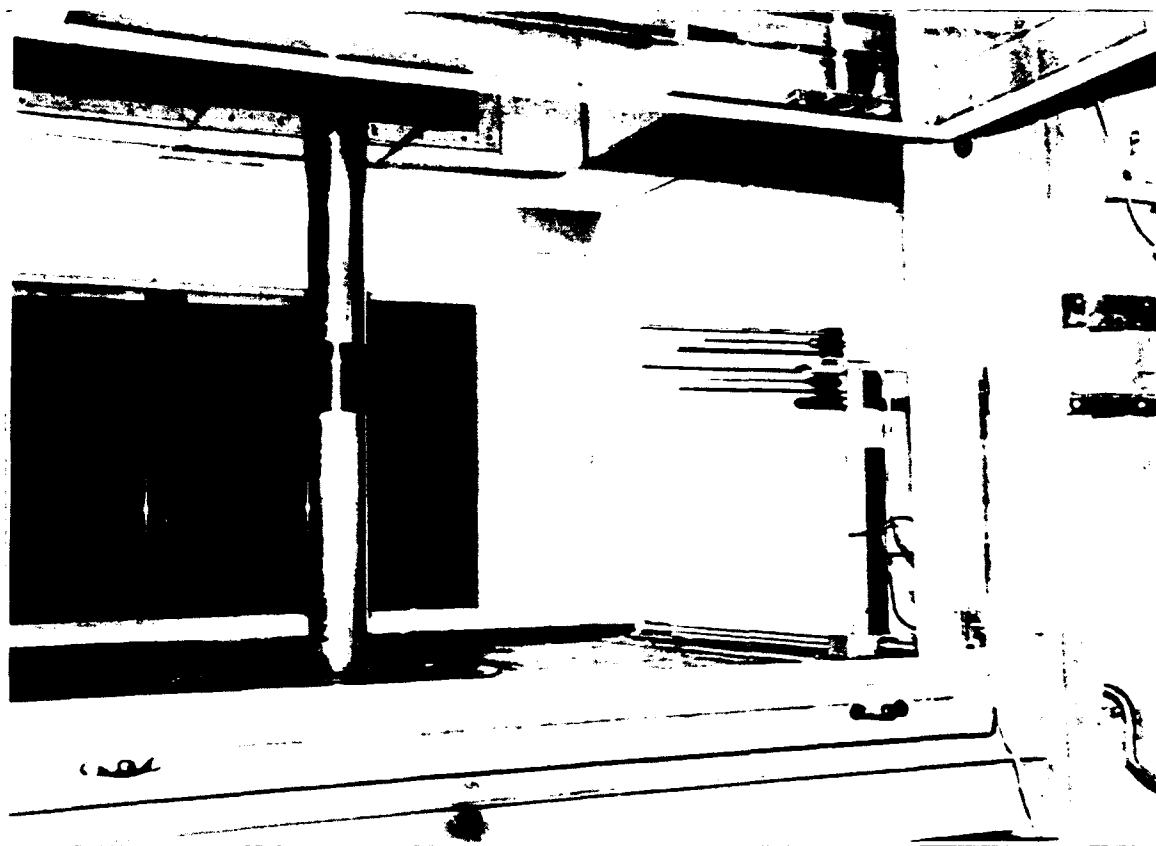


**Figure 1.** The Test Section Showing The Wake Traverse and Probes Apparatus

## **II. N.P.S. LOW SPEED WIND TUNNEL**

### **A. DESCRIPTION AND OPERATING PROCEDURES**

The NPS Laboratory Manual for Low Speed Wind Tunnel Testing [Ref. 1] provides an adequate discussion of the basic system description of the NPS Low Speed Wind Tunnel and its chief operating procedures and should be read thoroughly by all users. What follows is a summary of this description and those procedures of interest to the Cylinder Drag Experiment.

Figure 2 depicts the layout of the NPS Low Speed Wind Tunnel and the location of the test section. The wind tunnel is a closed-circuit, single-return type. It is powered by a 100 hp electric motor which drives a three-blade variable pitch fan.

A four-speed common truck transmission is used in-line with the motor and allows the wind tunnel to achieve tunnel speeds up to 200 MPH. The Cylinder Drag Experiment in AA2801 operates at approximately 115 MPH and for this, fourth gear is used. The contraction cone prior to the test section has a 10:1 contraction ratio which serves to increase the velocity of the airflow as well as causing the flow to become more uniform entering the test section.



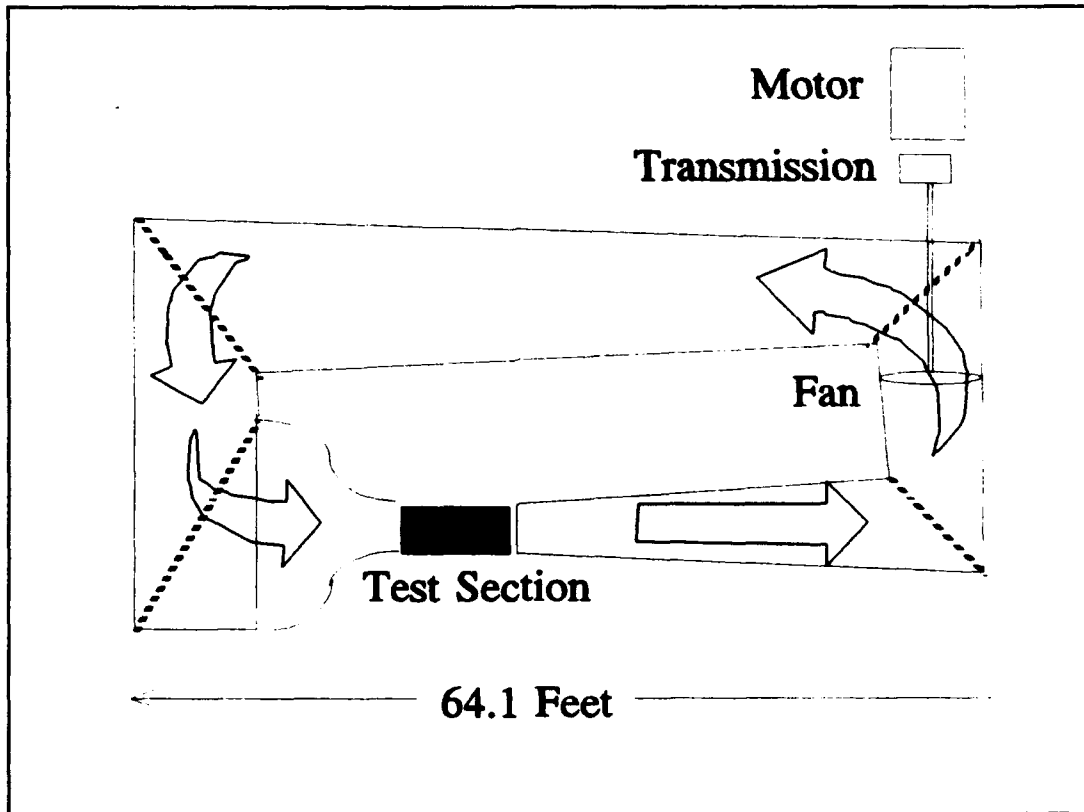


**Figure 2. NPS Low Speed Wind Tunnel**

The dimensions of the test section are given in Table 1.

**TABLE 1. Test Section Dimensions.**

length (l)	48.0 inches
width (w)	45.0 inches
height (h)	32.0 inches
total cross sectional area (C)	9.9 sq. ft
above the reflection plate:	
height ( $h_{eff}$ )	28.4 inches
cross sectional area ( $C_{eff}$ )	8.8 sq. ft

Figures 3 and 4 are views from inside the test section. The wind tunnel uses a water micromanometer to reference tunnel velocity by measuring  $\Delta p$ , the difference between two static pressures:  $p_1$  at the beginning of the contraction cone and  $p_2$  at the exit

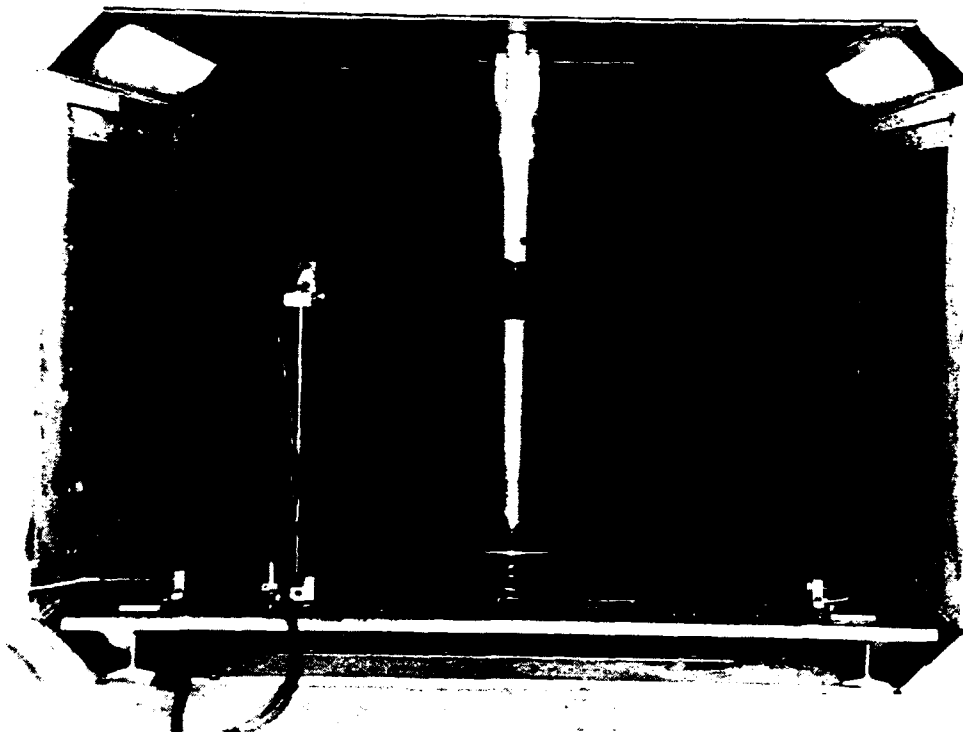


Figure 3. Test Section View - Into the Freestream

of the contraction cone. Since the airspeed is increased between the beginning and exit of the cone, there is a *decrease* in the static pressure as the air seeks to return to the lower ambient static pressure. This equalization is due to a breather slot, which allows ambient air to enter the circuit and mix with air leaving the test section. Hence,  $\Delta p$  changes primarily with increasing (or decreasing)  $p_1$ , as  $p_2$  remains essentially constant. Figure 5 shows the water micromanometer. Through calibration and associated equations and charts (see Section C), this  $\Delta p$  is related to airflow velocity.

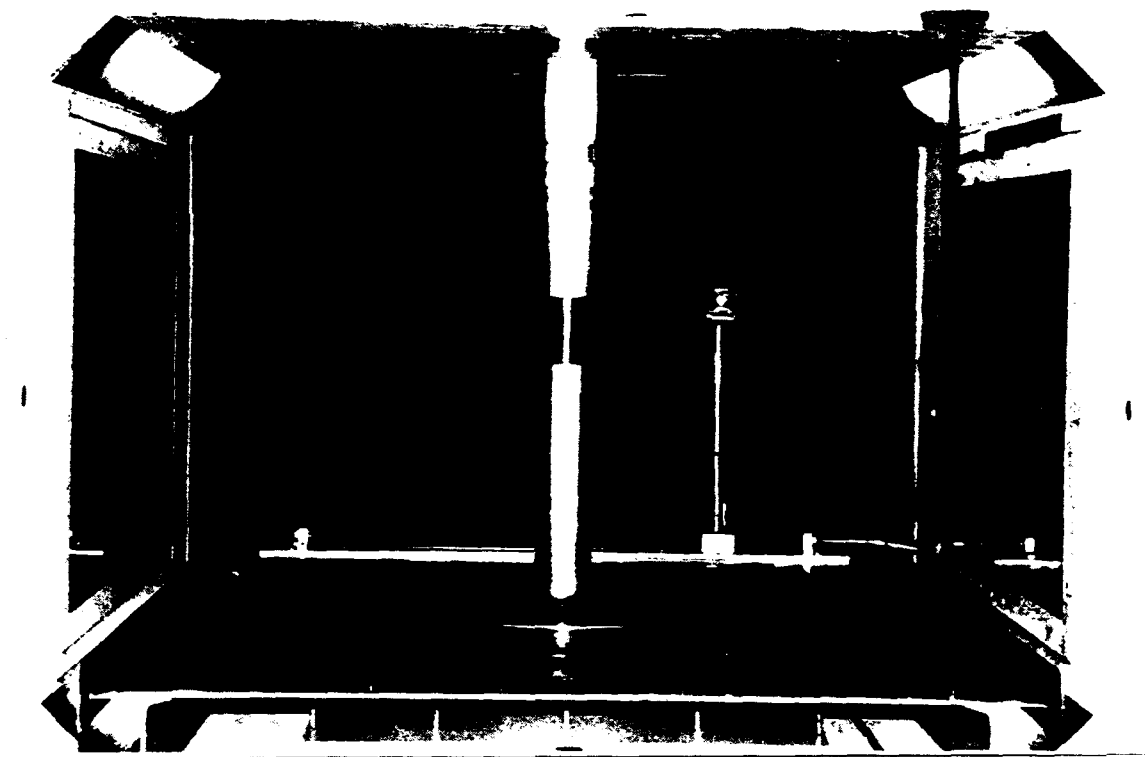


Figure 4. Test Section View - Looking Down Wind

Table 2 illustrates the operating instructions used during this lab.

**TABLE 2. Wind Tunnel Operating Procedures**

<b>STEP</b>	<b>PROCEDURE</b>
1	Decide on a required tunnel speed; convert to $\Delta p$ (H <sub>2</sub> O cm)
2	After confirming micromanometer reads 0.00 with tunnel fully stopped, set selected $\Delta p$ in window
3	Check tunnel doors closed and test section free from FOD; check transmission for proper gear; turn power switch to ON position
4	Depress and hold START button until green light goes out momentarily (meaning fan is turning and set to minimum pitch); release START button
5	Wait 5-10 seconds; depress COARSE UP button until water rises to enter the crosshair ring on micromanometer; toggle FINE UP/DOWN to maneuver meniscus to rest on crosshair; tunnel is set
STOP	Toggle COARSE DOWN until water level is below the 10 cm mark then momentarily depress STOP (button with red light); secure power switch; enter time into tunnel logbook
<b>EMERGENCY STOP:</b>	
Secure switch on red box near breather slot	

## **B. CORRECTION FACTORS**

Data taken from within the wind tunnel must first be corrected and calibrated due to the physical geometry of this particular wind tunnel. Of primary importance are the actual Reynolds number and dynamic pressure being experienced by an object inside the test section. Since these are functions of velocity, an accurate method of obtaining test section velocity must be available. This velocity may be derived from the difference  $p_1 -$

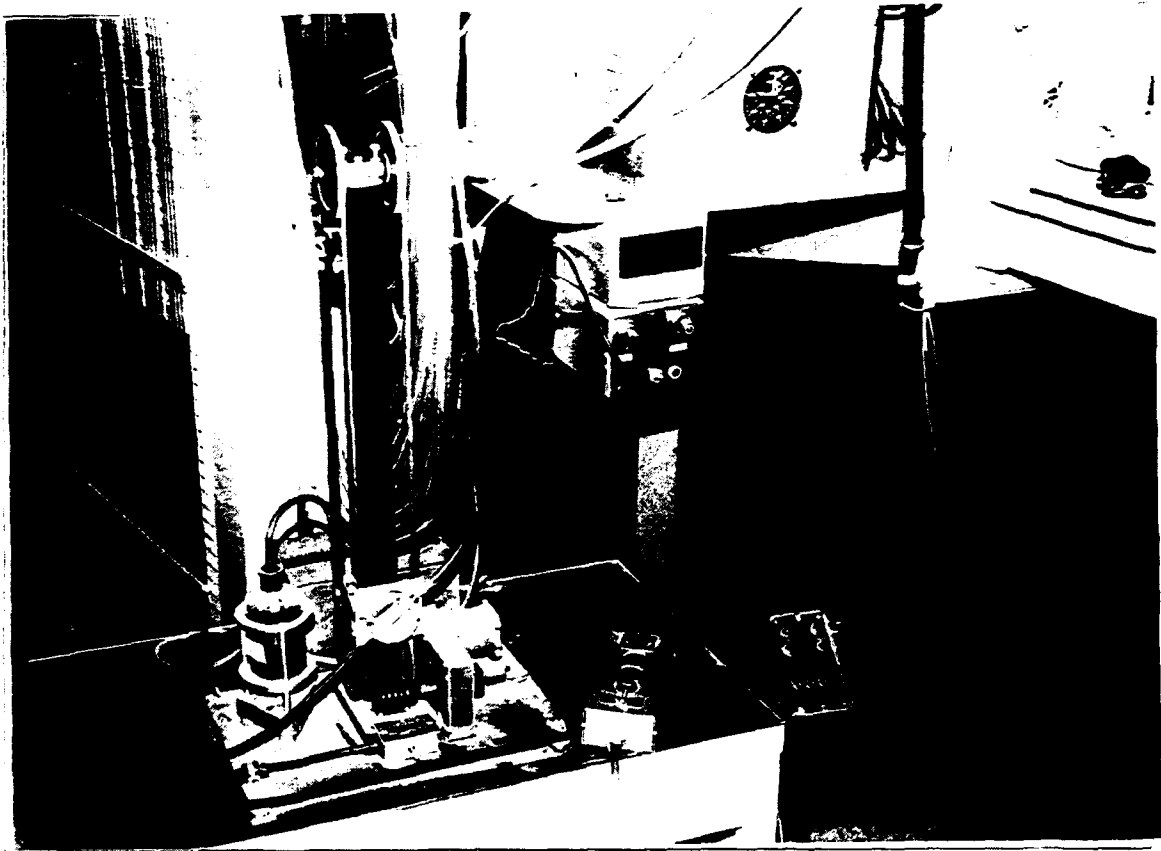


**Figure 5. N.P.S. Low Speed Wind Tunnel Water Manometer**

$p_2$ , but as was mentioned earlier, the tunnel  $\Delta p$  is meaningless unless it has first been *calibrated* to a known standard. This calibration procedure (which should be repeated before any important research is undertaken), is simply the tunnel calibration. The actual procedure and results are discussed in the next section. Here it is pointed out that  $\Delta p$ , once properly calibrated, may then be used to provide the test section freestream\*

---

\*"Freestream" will henceforth refer to any parameter measured in the test section which is unaffected by any object (eg. an airfoil) placed in or any mechanism directed into (eg. a jet of air) the test section, and will be shown with ( $\infty$ ) as the subscript.

velocity  $V_\infty$ , as demonstrated by equation (1). The development of the tunnel calibration equation is explained in the next section.

$$\Delta p = (\text{calibration factor}) \times q = (\text{calibration factor}) \frac{1}{2} \rho V_\infty^2 \quad (1)$$

Besides calibrating for  $q$ , there is a correction for the turbulence within the test section called the "Turbulence Factor," or  $TF$ . It is found experimentally and was not repeated for this thesis [Ref. 1:pp. 32-33].

$$TF = \frac{385,000}{Re_{CRIT}} \quad (2)$$

The  $TF$  was found experimentally for the NPS wind tunnel to be 1.04. The  $TF$  effectively raises the Reynolds number.

The final corrections of interest to this lab are the tunnel boundary corrections due to solid and wake blockage caused by the presence of the cylinder in the test section. These corrections account for the test section walls and the apparent "closed system" the data acquisition system experiences. These are corrections for two-dimensional testing. Solid blockage correction  $\epsilon_s$  compensates for increased velocity and dynamic pressure due to the blockage caused by the model [Ref. 1:p. 36].

$$\epsilon_{sb} = \frac{K_1 \cdot Volume}{C_{eff}^{\frac{3}{2}}} \quad (3)$$

$K_1$  is 0.52 for a model spanning the tunnel height and  $C_{eff}$  is the effective cross-sectional area of the test section.

The second factor is  $\epsilon_{wb}$ , or the wake blockage correction. The decrease in velocity caused by a wake results in an increased velocity outside the wake as the "closed system" tries to maintain a constant mass flow rate within the test section. This results in an increased dynamic pressure on the model. [Ref. 1:pp. 36-37]

$$\epsilon_{wb} = \frac{d}{2w} C_{du} \quad (4)$$

Here,  $d$  is the diameter of the cylinder,  $w$  is the width of the test section and  $C_{du}$  is the uncorrected drag coefficient. Reference 1 (pp. 36-37) goes into broader detail about what  $C_{du}$  represents. For the purposes of this experiment,  $C_{du}$  will be chosen to be  $c_d$  (and thus labeled " $c_{du}$ ") found by each of two methods described in the next chapter. Reference 1 offers a simple estimate for total blockage on page 37, so no significant loss in precision will be experienced in calculating  $c_d$ .

$$c_d = c_{d_u} (1 - 3\epsilon_{sb} - 2\epsilon_{wb}) \quad (5)$$

Thus [Ref. 1:p. 37],

$$\epsilon_{total} = \frac{K_1 \cdot Volume}{C_{eff}^{\frac{3}{2}}} + \frac{d}{2w} c_d \quad (6)$$

$\epsilon_{total}$  is then used in further corrections to velocity and the Reynolds number [Ref. 1:p. 38].

$$V = V_u(1 + \epsilon_{total}) \quad (7)$$

$$Re_{EFF} = Re_u(1 + \epsilon_{total})(TF) \quad (8)$$

### C. CALIBRATION AND RESULTS

The relationship between  $\Delta p$  and tunnel  $q$  is essentially linear and provides the tunnel calibration curve. The slope and intercept of the calibration curve comprise the tunnel calibration factor which is the object of the calibration.

The tunnel was calibrated on 26 April 1993 using three steps:

1. The output from a digital manometer was compared to that of a known standard and a correction factor was determined for the digital manometer.
2. The reading from the water micromanometer used for the wind tunnel ( $\Delta p$ ) was compared to that of the digital manometer, which now read wind tunnel  $q$  using a portable pitot-static tube placed in the center of the test section.
3. The data obtained were reduced to a plot of  $\Delta p$  versus corrected tunnel  $q$ ; this plot was the calibration curve sought.



### 1. Calibration Step One

The digital manometer was simply a transducer with one pressure port labeled "high" and one pressure port labeled "low." The high port was connected to the output of a known standard, in this case a device called the "Schmidter." Next, the manometer reading of the Schmidter was compared to the output of the digital manometer over the pressure range necessary for the test. The "Schmidter" is shown in Figure 6, and includes a cylinder which can be manually pressurized and a water manometer reading in centimeters.

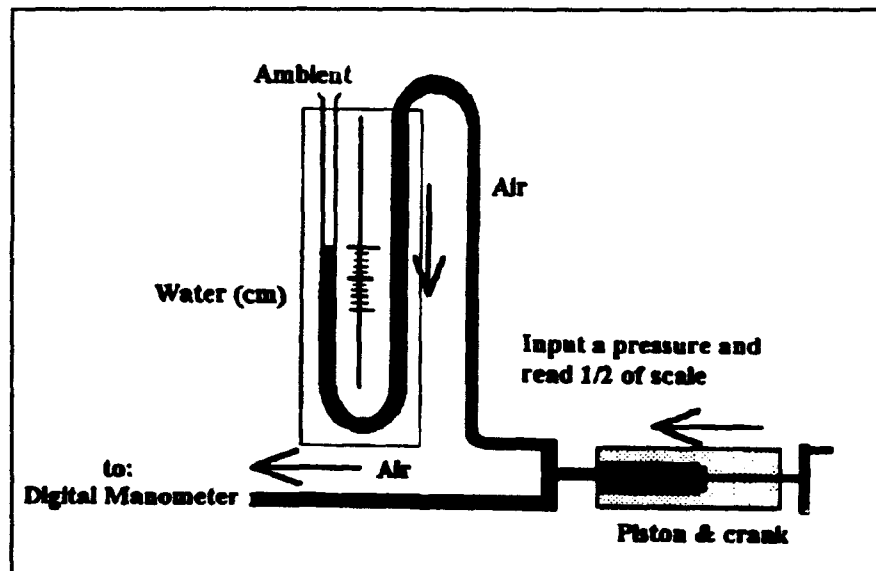


**Figure 6.** The "Schmidter" (a calibration manometer)

Two tests were made and the results were then averaged and plotted. Figure 7 shows the resulting conversion derived from this comparison. The subsequent slope and intercept (offset) of the plotted line were then applied to data found during step two.

Three things are to be noted concerning Figure 7: (1) the digital manometer was designed to read out in inches, not centimeters, and thus the conversion shown in Figure 7 shows inches; (2) it can be seen from the calibration equation in Figure 7 that the digital manometer had a linear error. This explains why the digital manometer had to first be calibrated to a known standard before it could subsequently be used to calibrate  $\Delta p$ ; and (3) finally, since the digital manometer used had an operating limit near 13 centimeters, higher runs were not pursued. Even though the calibration was not conducted at higher pressures, other data are available which ensure that the calibration factor remains linear for  $\Delta p$ 's above 13 centimeters. The AA2801 Cylinder Drag Experiment uses the wind tunnel in 4th gear at 15 cm  $H_2O$   $\Delta p$ .

## **2. Calibration Step Two**

The next step involved placing a standard pitot-static tube into the wind tunnel, extending approximately 10.5 inches from the top center of the test section and facing into the freestream. The tunnel was operated in increments of 1 cm  $H_2O$  (tunnel speed gauge ( $\Delta p$ )) and air velocity (in MPH) was recorded from the tunnel airspeed indicator. At each increment, the digital manometer output of the pitot-static tube was recorded (see Table 3). The tunnel was operated first in 4th gear, and then the operation was repeated in 3rd gear. The values read by the digital manometer were then averaged. The correction from Figure 7 was applied to this average and then plotted in Figure 8.

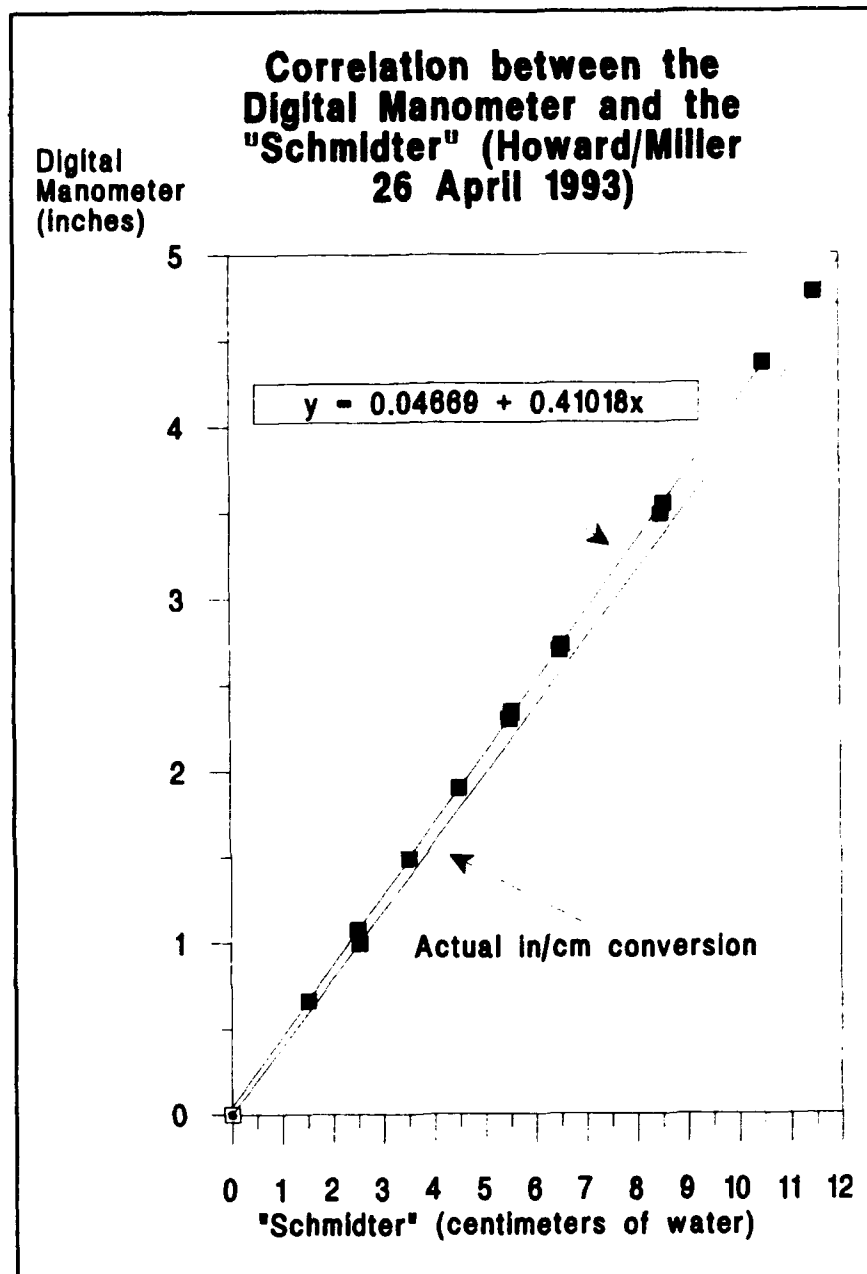


**Figure 7. Data From Step One of the Calibration**

**TABLE 3. Step Two Results**

First run in 4th gear/Second run in 3rd gear			Corrected q (cm)
$\Delta P$ (cm H <sub>2</sub> O)	Average Digital Manometer (inches)	MPH	
1.00	0.41	39	0.88
2.00	0.87	47	2.01
3.00	1.33	56	3.13
4.00	1.74	63	4.13
5.00	2.20	69	5.25
6.00	2.68	75	6.42
7.00	3.13	79	7.52
8.00	3.59	85	8.64
9.00	4.06	90	9.78
10.00	4.51	95	10.88
11.00	5.02	99	12.12
12.00	5.44	103	13.15

### 3. Calibration Step Three

Step three was to plot the first and fourth columns of data from Table 4 against each other. Again, a simple curve fitting program was used to find the calibration curve. Here, the slope and offset of Figure 8 provide the tunnel calibration factor, and the equation is  $0.243 + 0.895 * q$ , with q given in cm. of water. This differs from an earlier calibration of  $0.93 * q$ . It should be noted that the two formulas

are merely curve fits to measured data, and do not vary as much as might be supposed. The curves produce identical values at about 7 cm., and at 15 cm. only differ by about 0.25 cm. At 10 cm. the difference is about 0.1 cm., well within the fluctuation level of the micromanometer reading during the periodic pressure surges in the tunnel.

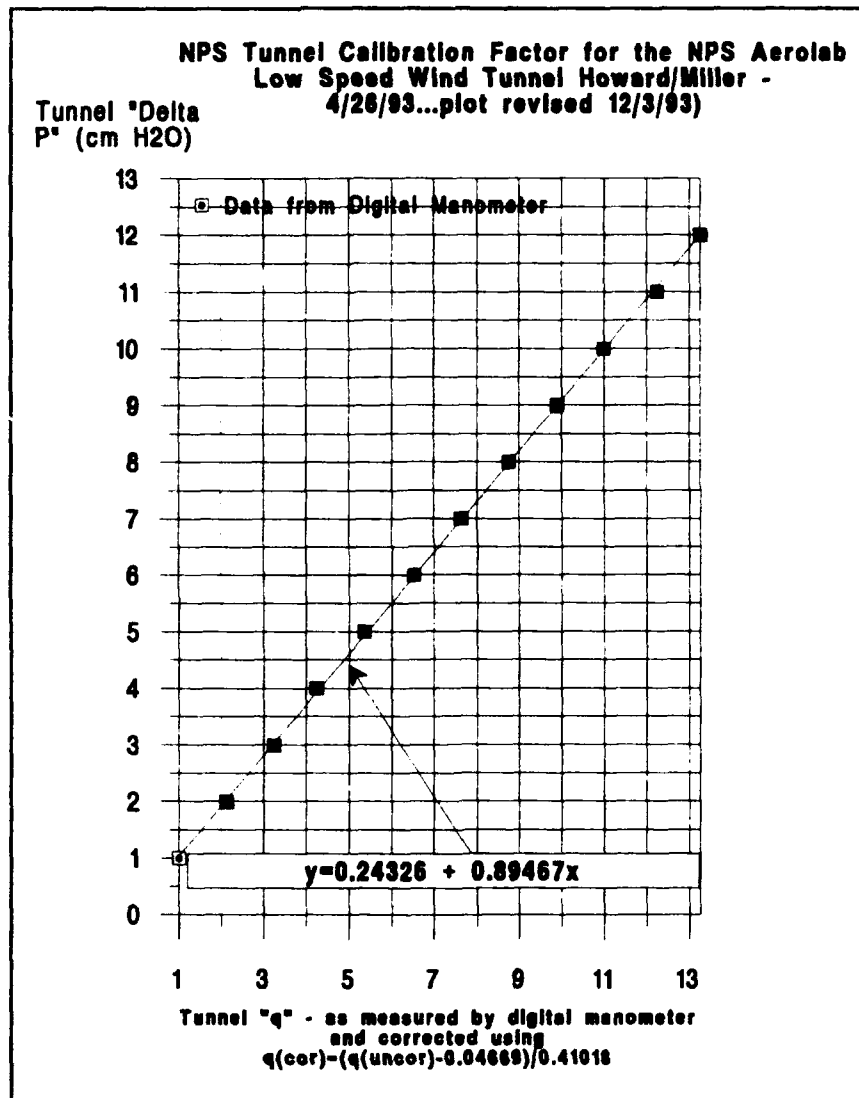


**Figure 8. Calibration Curve from Step Two data**

Dynamic pressure for incompressible flow is

$$\text{tunnel } q = q_{\infty} = \frac{1}{2} \rho_{\infty} V_{\infty}^2 \quad (9)$$

and  $\Delta p$  (in lb/ft<sup>2</sup>) is

$$\Delta p = [p_1 \text{ (cm)} - p_2 \text{ (cm)}](\gamma_{\text{water}})\left[\frac{1\text{ft}}{30.48\text{cm}}\right] \quad (10)$$

where

$$\gamma_{\text{water}} \approx 62.35 \frac{\text{lb}}{\text{ft}^3} \quad (11)$$

The wind tunnel calibration equation, from Figure 8, is

$$\Delta p = 0.243 \text{ (cm } H_2O) + 0.895 q_{\text{test section}} \quad (12)$$

And combining equations (9) through (12) and taking density  $\rho_{\infty}$  in slugs/ft<sup>3</sup>,

$$V_{\infty} \left( \frac{\text{ft}}{\text{sec}} \right) = \sqrt{\frac{2(\Delta p - 0.243)}{0.895 \rho_{\infty}}} \quad (13)$$

This equation has been written into a MATLAB code which uses different unit conversion factors to create updated velocity tables. This code is contained in Appendix E.

### III. CYLINDER DRAG THEORY

#### A. AERODYNAMIC DRAG CLASSIFICATION

From Reference 2:

TABLE 4. Drag Classification.

TOTAL DRAG - D		
SHEAR - $D_f$ (due to skin friction)  Dominates streamlined bodies	NORMAL (due to pressure)	
	Form - $D_p$ (due to separation)  Dominates blunt bodies	Induced (due to lift)
	Profile Drag = $D_f + D_p$ (2-D flow)	
	Parasite Drag = $D_f + D_p$ (3-D flow)	

Though not used in this experiment, a wind tunnel balance may be used to directly measure the drag (and lift/side) forces on a cylinder in the test section. The balances used are divided into two categories: internal (sting-type) and external. The NPS Low Speed Wind Tunnel has provisions for an external balance using a strain-gage bridge network which measures lift and drag.

Methods which use pressure to find drag include the pressure distribution method, which finds *form drag* only, and wake analysis, which finds *profile drag*.

## B. MEASURING DRAG BY PRESSURE DISTRIBUTION

### 1. Theory.

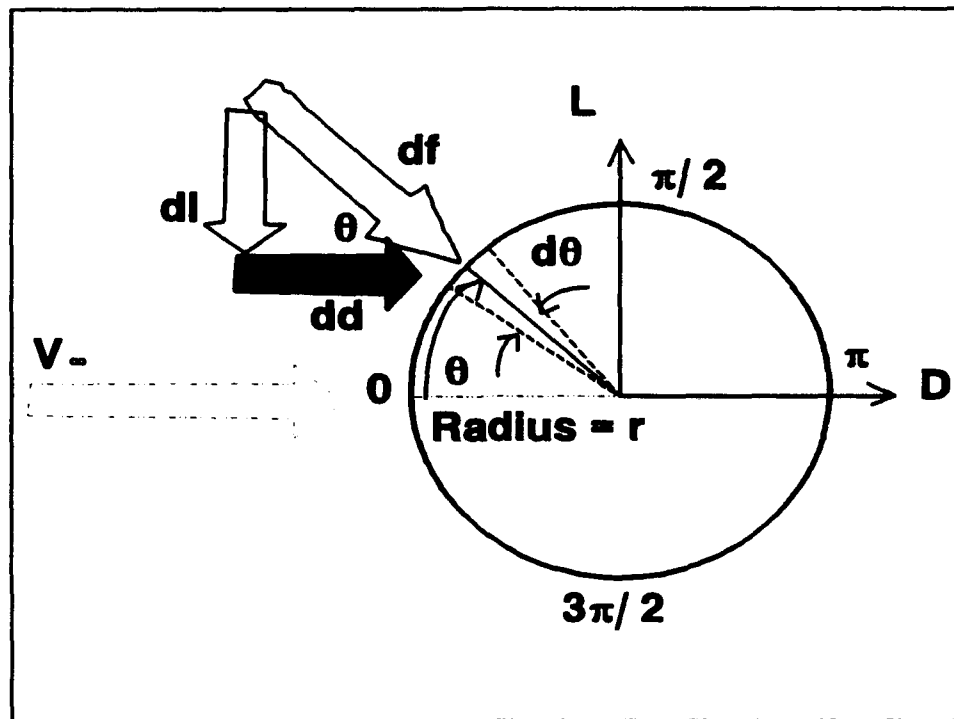


Figure 9. Pressure Forces on the Surface of a Cylinder

As shown in Figure 9, which was derived from a similar figure in Reference 3 (p. 58), there is a pressure force  $df$  acting normal to the surface of an airfoil. There is another pressure force not shown which acts tangentially to the surface. This tangential force is called shear and is a result of skin friction. However, for blunt bodies, drag related to surface pressure dominates and the tangential pressure force is commonly ignored [Ref. 3:p. 60]. So, the force shown is the significant contributor and has a



component called form drag  $dd$  associated with the streamwise drag acting on the cylinder. This form drag may be found by starting with the normal pressure force as follows:

$$df = p da = p (r d\theta) \quad (14)$$

where  $df$  is acting over a unit span and  $r$  is the radius of the cylinder, as shown. It follows that

$$dd = df \cos\theta = p r d\theta \cos\theta \quad (15)$$

where  $dd$  is the form drag component and  $dl$ , shown in Figure 9, is the induced drag component. By integrating over the whole surface of the cylinder to sum all the  $dd$  components,

$$\int_0^{2\pi} dd = r \int_0^{2\pi} p \cos\theta d\theta \quad (16)$$

which equals the *form drag*, or

$$D_p = r \int_0^{2\pi} p \cos\theta d\theta \quad (17)$$

The static pressure  $p$  acting normal to the cylinder's surface can be considered as a local static pressure which varies with the pressure port location (as the cylinder is rotated from  $\theta = -20^\circ$  to  $\theta = +180^\circ$ ) and the freestream static pressure which is constant. The freestream static pressure  $p_\infty$  can be pictured as a "blanket" of constant thickness enveloping all  $360^\circ$  of the cylinder. Integration of this "blanket" over a closed surface will result in zero.

As noted previously, integration of the local static pressure over the cylinder acting in the downstream direction will produce the form drag. Calling this local varying static pressure  $p_{cyl}$ ,

$$D_p = r \int_0^{2\pi} p_{cyl} \cos\theta d\theta \quad (18)$$

And due to symmetry,

$$\int_0^{2\pi} \cos\theta d\theta = 0 \quad (19)$$

which can be written due to constant  $p_\infty$ ,

$$r \int_0^{2\pi} p_\infty \cos\theta d\theta = 0 \quad (20)$$

Therefore, the part of the pressure which contributes nothing to the form drag can be removed from the previous expression:

$$D_p = r \int_0^{2\pi} p_{cyl} \cos\theta d\theta - r \int_0^{2\pi} p_\infty \cos\theta d\theta \quad (21)$$

which simplifies to

$$D_p = r \int_0^{2\pi} (p_{cyl} - p_{\infty}) \cos\theta d\theta \quad (22)$$

Furthermore, since the drag equation is already *per unit span*, it can now be made dimensionless. Also, as two-dimensional flow is being examined, the total reference area  $S$  reduces to the chord length  $c \times 1$ , which for the cylinder is  $2r \times 1$  and

$$C_{D_p} = \frac{D_p}{q_{\infty} S} \rightarrow c_{d_p} = \frac{r \int_0^{2\pi} (p_{cyl} - p_{\infty}) \cos\theta d\theta}{q_{\infty} 2r} \quad (23)$$

The  $r$ 's cancel, leaving

$$c_{d_p} = \frac{\frac{1}{2} \int_0^{2\pi} (p_{cyl} - p_{\infty}) \cos\theta d\theta}{q_{\infty}} \quad (24)$$

The pressure coefficient,  $C_p$ , is a dimensionless ratio between the local pressure acting normal to a given surface minus the freestream static pressure ( $p_{\infty}$ ), and the freestream dynamic pressure ( $q_{\infty}$ ). With reference to equation (24), since  $q_{\infty}$  at a fixed tunnel speed is simply a constant,

$$c_{d_p} = \frac{1}{2} \int_0^{2\pi} \left( \frac{p_{cyl} - p_{\infty}}{q_{\infty}} \right) \cos\theta d\theta \quad (25)$$

which is the same as

$$c_{d_p} = \frac{1}{2} \int_0^{2\pi} C_p \cos\theta d\theta \quad (26)$$

The cosine function is an even function and by symmetry the last equation can be written as

$$c_{d_p} = \int_0^{\pi} C_p \cos\theta d\theta \quad (27)$$

The following authors arrive at the same conclusions using slightly differing approaches:

1. Anderson, [Ref. 2:p. 209, equation 3.130]
2. Bertin and Smith, [Ref. 3:p. 59, equations 2.40, 2.42]
3. Rae and Pope, [Ref. 4: p.221, equation 4.29]
4. Hoerner, [Ref. 5:p. 1-9, equations 4-6]

There may be some concern regarding the sign convention used in this experiment as presented here. In the AA2801 Cylinder Drag Lab, it is assumed that  $\theta = 0$  and  $\theta = \pi$  are located as shown in Figure 9. Thus, integrating an otherwise dominating positive area yields a correspondingly positive  $c_{dp}$ . Classic discussion normally has the limits of integration reversed, with  $\theta = 0$  beginning at the leeward side of the cylinder and growing positive in a counterclockwise fashion. Additionally, after seeing a plot such as Figure 10, which compares theoretical (inviscid)  $C_p$  to actual (viscous)  $C_p$ , one might be led to believe that a negative sign would be required in front of Equation (27) just to make  $c_{dp}$  positive.

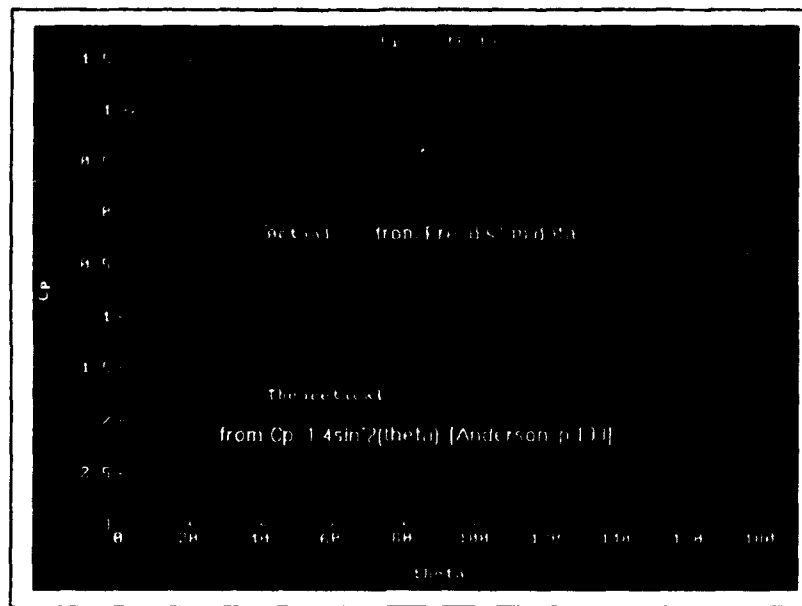


**Figure 10.** Inviscid  $C_p$  as Compared to Actual  $C_p$

Actually, the integrand is not *simply*  $C_p$ ; it is  $C_p \sim \cos\theta$ . Figure 11 makes this apparent and addresses the positive-area/positive sign question.

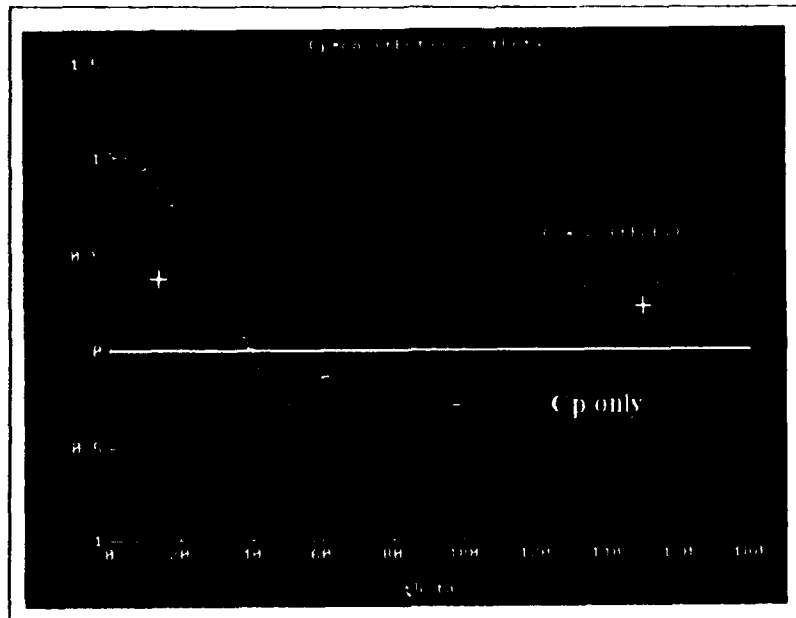


Figure 11.  $C_p \cos \theta$  compared to  $C_p$

## C. MEASURING DRAG BY WAKE ANALYSIS (MOMENTUM)

### 1. Theory

In Reference 6 (p. 66), steady 1-D flow (as in a wind tunnel test section with no flow distortion) can be represented by the momentum equation:

$$\sum \bar{F} = \frac{(\text{mass flow rate})}{g_c} (\bar{V}_{out} - \bar{V}_{in}) \quad (28)$$

Drag, by definition, is a negative component of  $\sum \bar{F}$ , so swapping  $V_{out}$  and  $V_{in}$  in equation (28) will keep their difference a positive value. The flow behind the cylinder,

for purposes in this laboratory, is two-dimensional. Rae & Pope develop the momentum equation [Ref. 4:p. 214] into a double integral and state that "...the part of the air that passes over the model suffers a loss of momentum, and this loss is shown by and equal to the profile drag..." Profile drag, as mentioned earlier, is two-dimensional drag composed of both skin friction ( $D_f$ ) and form drag ( $D_p$ ), and is collectively denoted here as  $D$ . Thus, since mass flow rate equals  $\rho AV$ , where  $A$  is the area of the wake perpendicular to the freestream,

$$D = \iint \rho V_w dA (V_\infty - V_w) \quad (29)$$

In incompressible (low speed) theory,  $\rho_w$  equals  $\rho_\infty$  (*a constant*) and the equation becomes

$$D = \iint (\rho_\infty V_\infty V_w - \rho_\infty V_w^2) dA \quad (30)$$

For a unit span of the cylinder, as was explained earlier,  $S$  equals  $c \times 1$  equals  $2r \times 1$ , and for a unit slice of the wake along the  $y$ -axis,  $Da$  equals  $dy \times 1$ . So two-dimensional drag, denoted by  $d$  may be written

$$d = \int [\rho_\infty V_\infty V_w - \rho_\infty V_w^2] dy \times 1 \quad (31)$$

Since

$$C_D = \frac{D}{q_\infty S} \quad (32)$$

then

$$c_d = \frac{d}{q_\infty (c \times 1)} = \frac{d}{(\frac{1}{2} \rho_\infty V_\infty^2) 2r} = \frac{d}{(\rho_\infty V_\infty^2) r} \quad (33)$$

and substituting equations (31) into (33) yields

$$c_d = \frac{\int [\rho_\infty V_\infty V_w - \rho_\infty V_w^2] dy}{\rho_\infty V_\infty^2 r} \quad (34)$$

The densities cancel out and since the rest of the denominator is also a constant, then

$$c_d = \frac{1}{r} \int \left[ \frac{V_\infty V_w}{V_\infty^2} - \frac{V_w^2}{V_\infty^2} \right] dy \quad (35)$$

Equation (9) from page 17 may be rewritten as

$$V_\infty = \sqrt{\frac{2q_\infty}{\rho_\infty}}, \text{ while } V_w = \sqrt{\frac{2q_w}{\rho_\infty}} \quad (36)$$



Substituting equation (36) into equation (35) yields,

$$c_d = \frac{1}{r} \int \left[ \sqrt{\frac{q_w}{q_\infty}} - \frac{q_w}{q_\infty} \right] dy \quad (37)$$

Since  $q_w$  and  $q_\infty$  are simply  $((p_0)_w - p_w)$  and  $((p_0)_\infty - p_\infty)$ , the difference between these two ratios are then integrated over the width of the wake to get

$$c_d = \frac{1}{r} \int_0^{20} \left[ \sqrt{\frac{p_{0w} - p_w}{p_{0\infty} - p_\infty}} - \frac{p_{0w} - p_w}{p_{0\infty} - p_\infty} \right] dy \quad (38)$$

Similar results to those in the previous analysis were obtained by:

1. Anderson, [Ref. 2:p. 107, equation 2.74]
2. Rae and Pope, [Ref. 4:p. 215, equation 4.24]
3. Hoerner, [Ref. 5:p. 1-7]
4. Panton, [Ref. 9:p. 386]

## **IV. AA2801 CYLINDER LAB**

### **A. PREVIOUS LABORATORY**

#### **1. Procedures**

The former laboratory procedures for the AA2801 "Drag on a Cylinder" may be found in Reference 7 and are reproduced in Appendix A for contrast.

#### **2. Limitations and Problems**

##### ***a. Limited Data Acquisition***

Chief among the limitations of the previous lab was the lack of numerical data. Thus, all analysis was strictly drawn from graphs made by the Hewlett-Packard X-Y Plotters (see Figure 12). Students would count squares under the curves, assign coordinates to the curve, use a planimeter to measure the area under the curve, and one student was even known to cut out the curves and a small representative square and then weigh them on a precision digital scale! Also, not being able to retrieve data meant that this lab served only one real purpose: Estimating Drag on a Cylinder. Certainly the potential to expose students to the functional use of the wind tunnel existed but was not exploited by this approach. Beyond the lack of data retrievability, there were other problems with the former lab procedures.

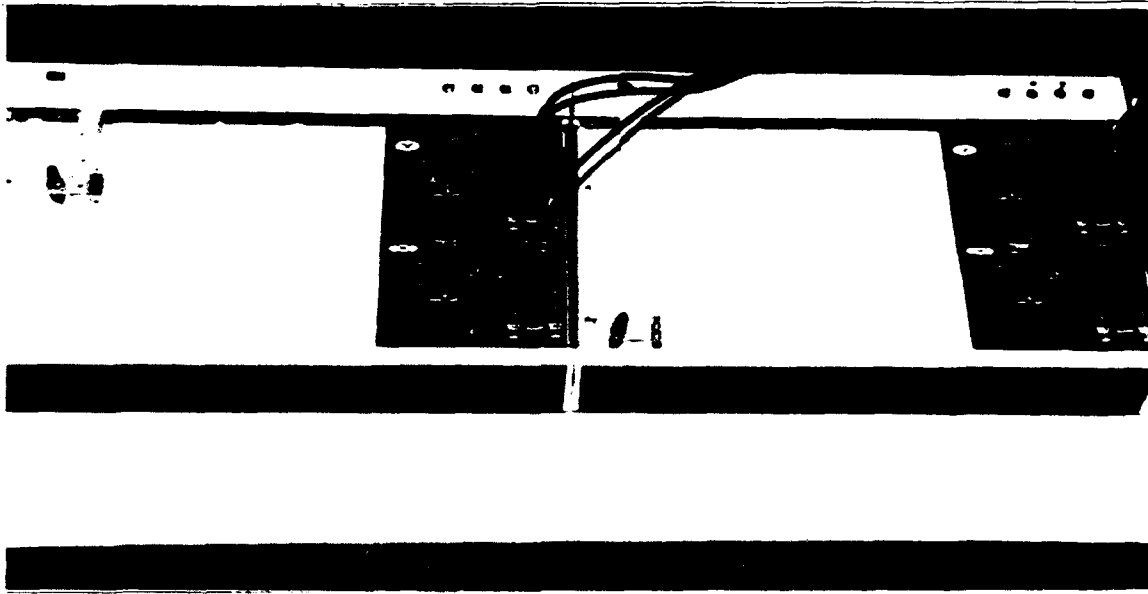


Figure 12. Hewlett & Packard X-Y Plotters.

*b. Poor Relation Between Method Chosen and Actual Procedures*

The wake analysis equation given in the old lab,

$$C_d = \frac{2}{d} \int \left[ \frac{V_2}{V_1} - \left( \frac{V_2}{V_1} \right)^2 \right] \delta y - \frac{1}{d} \int \left[ \frac{P_2 - P_1}{q_1} \right] \delta y \quad (39)$$

was supposed to have been derived from Newton's Second Law using the Reynold's [sic] Transport Theorem. To further complicate things, the lab had students allegedly plotting two (but not all three) parts of this equation. These two parts were:

$$(V_2/V_1)^2 \text{ vs. } y \text{ and } (P_2 - P_1)/q_1 \text{ vs. } y.$$

Next, the students were to subtract one curve from the other to estimate  $C_d$  (not written as " $c_d$ "). To begin with, the equation does not agree with contemporary definitions of the wake analysis method (see Chapter III, Section C). Secondly, the procedure does not support the equation - either intuitively or precisely. While it was

pointed out that  $(V_2/V_1)^2$  was simply  $q_2/q_1$ , the  $V_2/V_1$  portion was missing. Also, subtracting one curve from another does not lead to the solution of the equation given. Finally, the  $P_2 - P_1$  values do not represent anything useful.  $P_2$  was the static source in the wake while  $P_1$  was the static port on the cylinder directed into the freestream at  $\theta$  equals  $0^\circ$ . The difference, measured this way, was between the static pressure through the wake and the stagnation pressure at the cylinder. This was confusing and bothersome for an otherwise simple method of drag estimation.

*c. Complexity of Procedures and Sparsity of Educational Value*

To make the plot described above, the student had to crank the traverse over and back while the technician had to change leads into the X-Y plotter. Graph paper had to be placed properly and the technician was inordinately relied upon to make the lab work. The student played a minor role in the lab other than observation and cranking. Perhaps one of the more valuable parts of the experiment, the setting of the scale of the transducers, was left to the technician. Additionally, the student learned very little about data acquisition, something that would greatly benefit him or her for future use of the wind tunnel. The lab handout provided sparse information for answering the question, "Why?"

*d. Inconsistency/Inaccuracy of Terminology*

$P_1$  was never defined, nor was  $q_1$ . " $C_d$ " was used for two-dimensional flow where " $c_d$ " is the convention used by most texts. The length of the cylinder was given as 28.0 inches when it is actually 28.4 inches, which changes the volume from

192.68 in<sup>3</sup> to 195.43 in<sup>3</sup>. The pitot probe and the static probe on the traverse were referred to as "two pitot-static probes."

## B. UPGRADED LABORATORY

### 1. Data Acquisition and System Description

#### a. Schematic

Figure 13 illustrates the signal path for the AA2801 Cylinder Drag Lab upgrade. Meanwhile, the photograph in Figure 14 is significant: data acquisition, data storage, data retrieval and data reduction - all in one place.

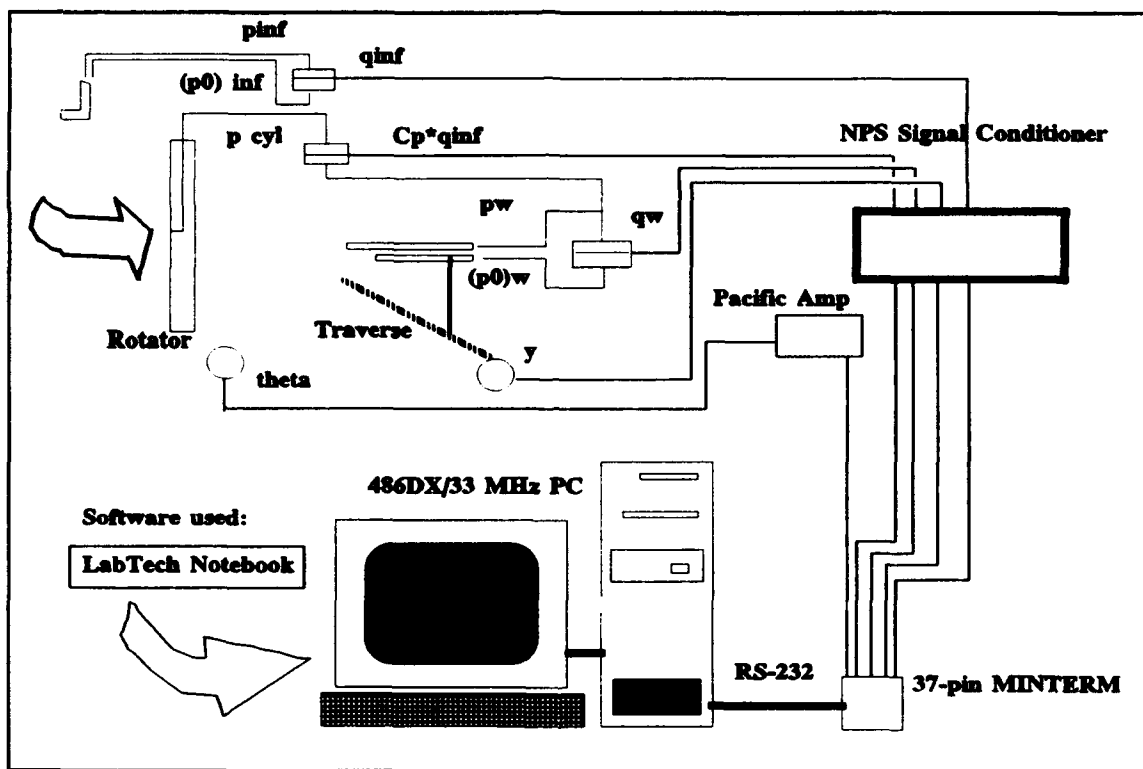


Figure 13. Signal Path of Data Acquisition System



**Figure 14.** 486DX/33 MHz PC Used For Data Acquisition

**b. Signal Configuration**

(1)  $p_{cyl} - p_w$ . There are two static pressure ports: a local pressure port ( $p_{cyl}$ ) located on the surface of the cylinder approximately mid-height and a static pressure port ( $p_w$ ) located on a traverse probe mount. Both pressures feed into a Statham pressure transducer rated at  $\pm 1$  psid, 15 Vdc maximum input. The transducer is excited by approximately 11 volts and the output signal is then fed to an NPS-built signal conditioner, and then on to the PC.

(2)  $(p_o)_w - p_w$  equals  $q_w$ . Traverse mounted pitot and static probes ( $(p_o)_w$  and  $p_w$ ) are co-located behind the cylinder and the pressure measured from these are fed into a Statham transducer, Model P69-1D-350 rated at  $\pm 1$  psi. The signal path to transducer and to the PC is identical to that of the previous transducer.

(3)  $y$ . A mechanical traverse operated by a hand-crank moves the mount which holds the pitot and static probes behind the cylinder. A small gear drives a 10-turn, 50K  $\Omega$  IRC potentiometer, Type H115-T-5620. The potentiometer is excited with approximately 11 volts and the output signal is fed from the NPS-built signal conditioner to the PC.

(4)  $\theta$ . The cylinder is mounted to a turntable, with rotating gear driving an Amphenol 100  $\Omega$ , 10-turn potentiometer, Type 4301 B. The potentiometer is excited by 0.56 volts while the output signal is fed to a Pacific Amplifier/Signal Conditioner, Model 8255 and amplified 100 times before routing to PC. The location of the turntable's azimuth scale is such that the cylinder local pressure port is pointing

directly into the freestream when  $\theta$  equals  $0^\circ$ . The turntable rotates the cylinder clockwise from  $\theta = -20^\circ$  to  $\theta = +180^\circ$ . Figure 15 shows the rotatable base.

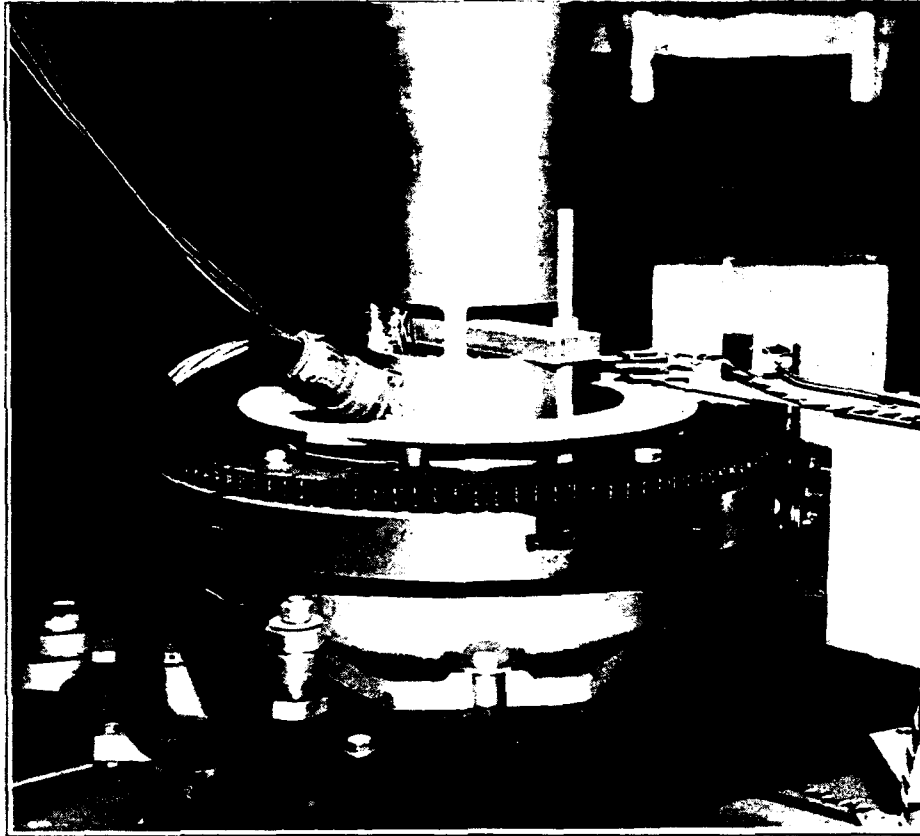


Figure 15. Electrically Rotatable Base for Cylinder

(5)  $(p_0)_\infty - p_\infty$  equals  $q_\infty$ . The tunnel airspeed indicator pitot-static tube, located under the ceiling in the forward part of the test section, is used to provide  $(p_0)_\infty$  and  $p_\infty$  to a Statham pressure transducer rated at  $\pm 1$  psid, 15 Vdc maximum input. This transducer is excited by approximately 11 volts and returns its output to an NPS-built signal conditioner (shown in Figure 16), then to the PC. The airspeed indicator serves as a reference static pressure under the assumption that  $p_\infty$  read there remains essentially constant at a fixed  $\Delta p$ , as was verified by calibration.



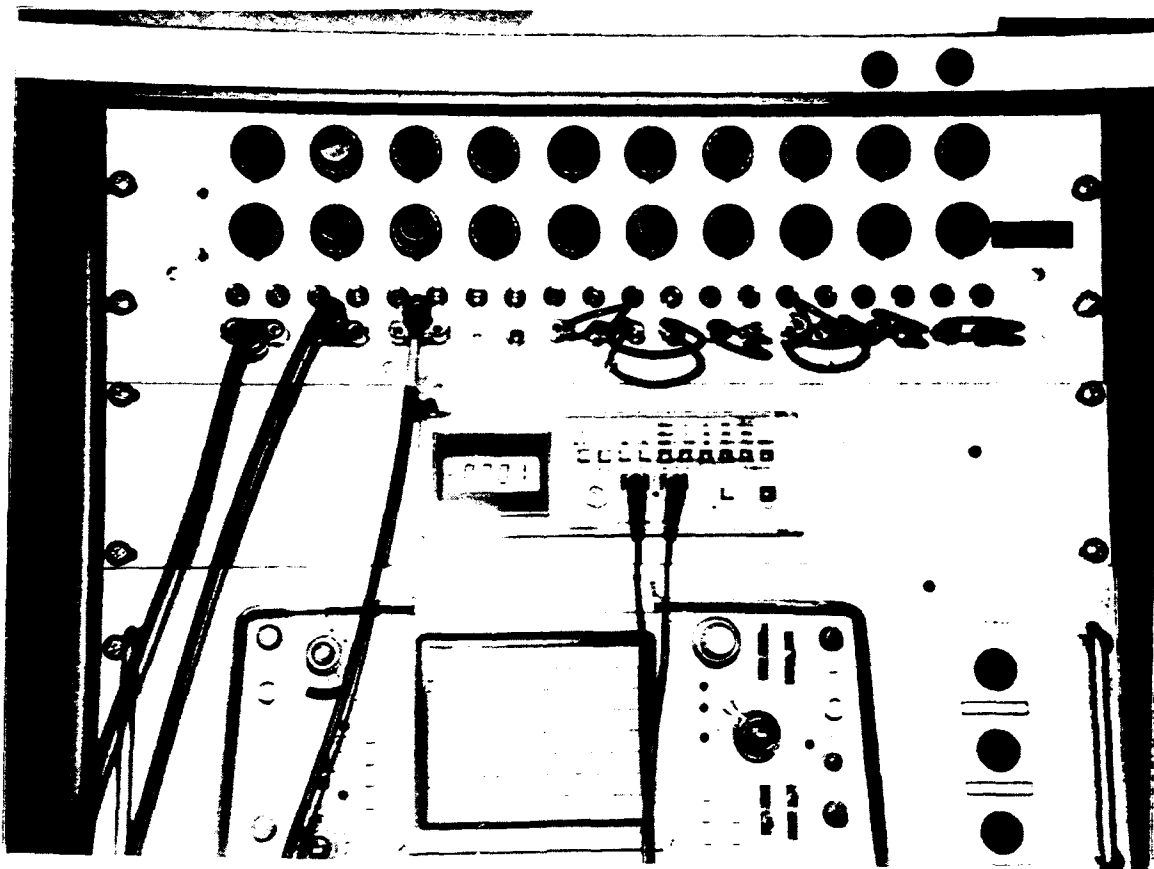


Figure 16. N.P.S. Signal Conditioner

(6) *CIO 37-pin MINITERM Connector Board.* All signals arrive here first and are attached via "channel" points to a standard 37-pin RS-232 cable (see Figure 13).

(7) *ComputerBoards CIO-DAS16/330 A/D Card.* A high-speed analog and digital data acquisition card was placed in the PC with a base address of 300H (300 HEX). A special library in the software package allowed the computer to use the A/D card (see Appendix B).

(8) *IBM 486DX/33 MHz PC.* A standard 486 IBM-clone PC was the terminal for the data acquisition system. This PC had DOS version 5.0 and Windows version 3.1 loaded.

*c. Software*

LabTech Notebook for Windows, version 7.1.1, was the operating software used to drive the data acquisition system. It is a process and control type application which can be used to both collect data and to control systems.

LabTech Notebook has two basic operating modes: BUILD-TIME and RUN-TIME. As their titles imply, BUILD-TIME is used to construct *set-ups* which are then executed in RUN-TIME. These set-ups contain customized "ICONblocks" which connect signals and create displays and data files.

**2. "ZERO" and "SPAN"**

These two LabTech Notebook set-ups were created to handle the job of scaling the signals coming into the program. It was felt that the signals must be correct, not just leaving the signal conditioners, but more importantly, entering the PC. Noise and other anomalies affect the signal at all points in its path. ZERO and SPAN are fully explained in Appendix B.

**3. Procedures**

*a. Run #1 - Pressure Distribution Method*

(1) *Approach.* While maintaining the reference static pressure  $p_w$  outside the wake and behind the cylinder (which is thus  $p_\infty$ ), the cylinder is rotated at a constant rate (and so is  $p_{cyl}$ ) from  $0^\circ$  to  $+180^\circ$ . The turntable is started at  $\theta = -20^\circ$  to ensure any acceleration is essentially zero by the time it passes  $\theta = 0^\circ$  and the maximum  $p_{cyl}$  is actually recorded, although this is not required.

(2) *Measured sources.* The signals being measured were  $p_{cyl} - p_w$  v.  $\theta$ , where  $p_w$  is the reference pressure and is assumed to be the freestream static pressure ( $p_\infty$ ) of the test section and where  $\theta$  is the position of  $p_{cyl}$ , the local static pressure on the cylinder, as it varies from the stagnation pressure, through  $p_\infty$ , past the point of maximum velocity, past the separation point of the boundary layer and finally to  $\theta$  equals  $180^\circ$ .

(3) *Purpose.* These measurements will be used by the software to find and plot  $C_p$  v.  $\theta$ .

(4) *Signal scaling criteria.* Before running the tunnel, at zero tunnel  $\Delta p$ , since  $q$ ,  $p_{cyl}$ ,  $p_\infty$ ,  $p_w$  and  $C_p$  all equal 0, the transducer output is conditioned to also read 0.00 volts. Next, the tunnel is run at 15 cm.  $H_2O$ , with  $\theta$  equal to  $0^\circ$  and  $y$  equal to 0.0 inches. But at  $\theta$  equals  $0^\circ$ ,  $p_{cyl}$  equals  $(p_0)_\infty$ . Since it is known that

$(p_0)_\infty$  equals  $q_\infty + p_\infty$ , the following substitution can be made for  $C_p$ :

$$\text{at } \theta = 0^\circ, C_p = \frac{(q_\infty + p_\infty) - p_\infty}{q_\infty} = \frac{q_\infty}{q_\infty} = 1.0 \quad (40)$$

Knowing this, the output signal can be conditioned for the transducer to read 0.01 volts.

The software used on the PC is then simply configured to multiply the signal coming in by 100 so that 0.01 volts is displayed as 1.0 when  $C_p$  actually equals 1.0. Figure 17 illustrates the LabTech Notebook set-up "PRE\_DIS1." Figure 18 shows the actual

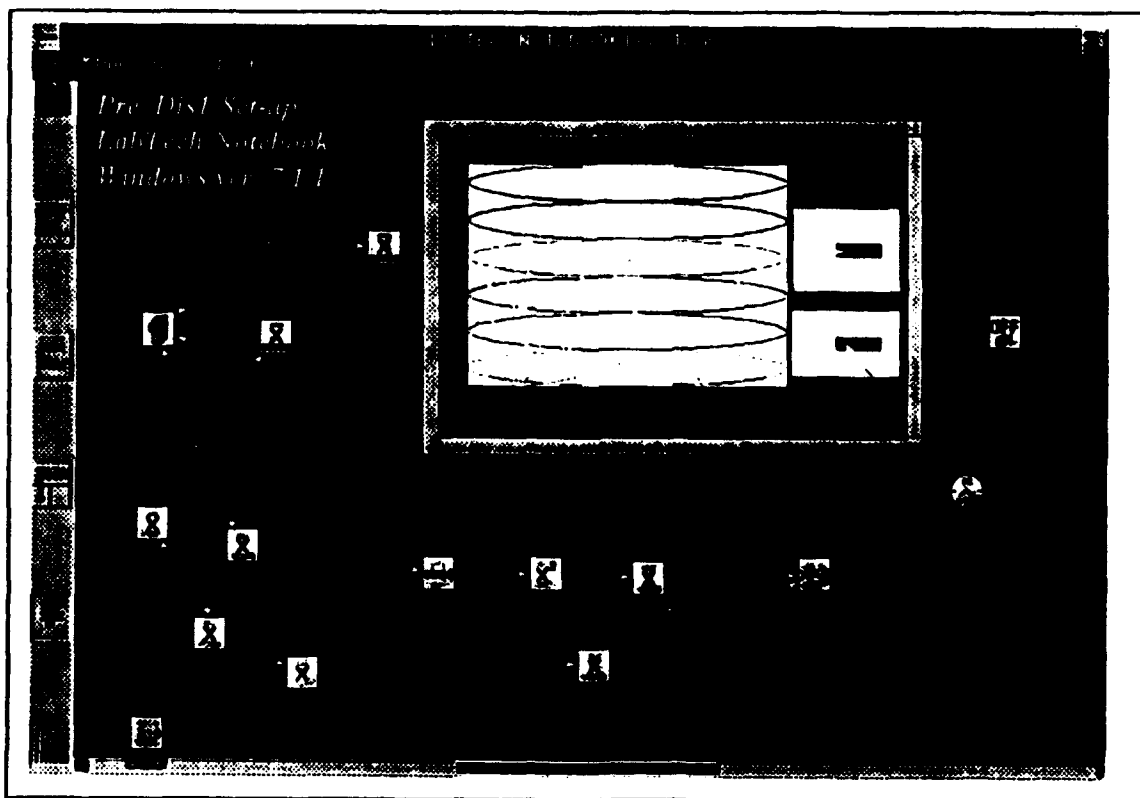
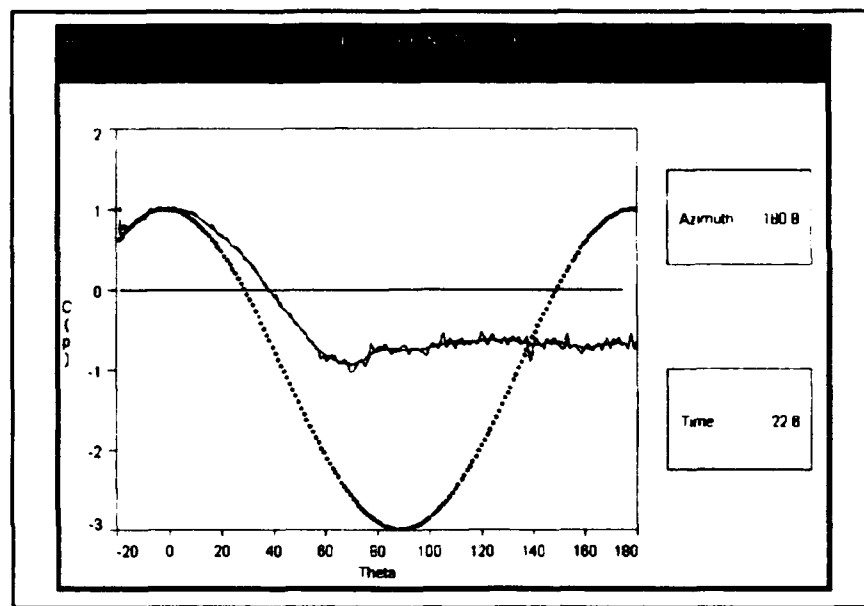


Figure 17. LabTech Notebook Set-Up "PRE\_DIS1"

results of executing PRE\_DIS1 in RUN-TIME.

(5) *Expected results.* From inviscid, incompressible theory, the pressure distribution method will generate a cosine-type curve starting out with  $C_p$  equal to 1.0 at  $\theta$  equal to  $0^\circ$  and decreasing through  $C_p$  equal to 0 to a minimum of  $C_p$  equal to -3.0 or separation, whichever occurs first (see Figure 18).



**Figure 18.** Actual LabTech Notebook Readout of  $C_p$  vs.  $\theta$  from Run #1

The point of separation will also define the point of wake initiation. It is anticipated that the wake behind a stationary cylinder in moving fluid, where the Reynolds numbers are of the order  $2.7 \times 10^5$ , will not change appreciably in width (in the y-direction) from where it begins [Ref. 2:p. 238, Fig. 3.40d]. As the wake progresses in the x-direction away from the cylinder, it seeks to recover back to the freestream condition. Thus, the

width of the wake, for this Reynolds number, may be *approximated* by entering the value for azimuth at the point of separation into the following equation:

$$\text{maximum expected wake width } (y'_{\text{wake}}) \approx 2 ( d | \sin \theta | ) \quad (41)$$

where  $d$  is the diameter of the cylinder in inches. This value was used to predict the beginning of the wake during Run #2.

(6) *Using the data obtained during data acquisition to estimate the drag coefficient.* Using the pressure distribution method for blunt bodies, form drag is the significant contributor to the resultant force on a non-rotating cylinder in airflow [Ref. 3:pp. 59, 60], [Ref. 2:p. 60, 209]:

$$c_{d_p} = \int_0^\pi \frac{p-p_\infty}{q_\infty} \cos\theta \, \delta\theta, \text{ where } C_p = \frac{p-p_\infty}{q_\infty} \quad (42)$$

The data obtain during Run #1 is a column of raw  $C_p$  values, a column of corresponding azimuth ( $\theta$ ) values, and a column of theoretical  $C_p$  values, the latter of which are obtained from the equation for theoretical inviscid, incompressible surface pressure coefficients over a cylinder [Ref. 2:p. 199]:

$$C_p = 1 - 4\sin^2\theta \quad (43)$$

Having these data, any program or technique of integrating the first two columns over the interval of 0 to  $\pi$  will supply the value  $c_{d_p}$ . Tabular data were not available in previous labs and students relied on physically measuring the area under

the curve from 0° to +180°. Now, using LabTech Notebook and automatic data acquisition, data are stored in an ASCII file and may be imported into a program such as MATLAB for analysis.

To compare the  $c_{dp}$  obtained from the experiment to empirical data, the Reynolds number is calculated from

$$Re = \frac{\rho_{\infty} V_{\infty} d}{\mu_{\infty}} \quad (44)$$

and the graph of Re vs.  $C_D$  shown in Reference 7, (p. 36) or Figure 24 is used. Care must be taken to correct Re for the turbulence factor, TF, to produce the effective Re:

$$Re_{EFF} = Re_{uncorrected}(1+\epsilon) \cdot TF \quad (45)$$

where

$$\epsilon = \epsilon_{sb} + \epsilon_{wb} \quad (46)$$

***b. Run #2 - Wake Analysis Method***

(1) *Approach.* While the cylinder is fixed in some (any) position  $\theta$ , the wake probes are moved along a y-axis traverse from 0.0 inches to +20.0 inches.

(2) *Measured sources.* Three values are measured during this run:  $q_w$ ,  $q_\infty$ , and traverse location,  $y$ . By definition,  $(p_0)_w - p_w$  equals  $q_w$  and  $(p_0)_\infty - p_\infty$  equals  $q_\infty$ . It has been shown experimentally that when the probes which measure  $(p_0)_w - p_w$  are located outside the wake,  $q_w$  equals  $q_\infty$ . Since  $q_w/q_\infty$  is the ratio sought, the wake analysis (momentum) method is really used to determine variations in velocity through the wake.

(3) *Purpose.* These values will be used by the software to plot the following difference in ratios:

$$\sqrt{\frac{(p_0)_w - p_w}{(p_0)_\infty - p_\infty}} - \frac{(p_0)_w - p_w}{(p_0)_\infty - p_\infty} \quad v. \quad y \quad (47)$$

which is

$$\sqrt{\frac{q_w}{q_\infty}} - \frac{q_w}{q_\infty} \quad v. \quad y \quad (48)$$

The difference between these two ratios forms the integrand of the momentum method for calculating the drag coefficient, as was explained earlier.

(4) *Signal scaling criteria.* Before running the tunnel, at zero tunnel delta P, all pressures are equal, all  $q$ 's are zero and all transducer outputs are scaled to read 0.0 volts. Next, the tunnel is run at 15 cm H<sub>2</sub>O, with  $y$  equal to 0 inches. Here, outside the wake,  $q_w$  equals  $q_\infty$  (both  $\neq 0.0$ ). Since  $q_w/q_\infty$  will be plotted, using the



Commutative Law, both outputs are scaled to the same value, in this case 1.0. Actually, any common value would have worked since the ratio when  $q_w$  equals  $q_\infty$  is *always* unity.

Figure 19 shows the set-up WAKE\_AN1/2 from LabTech Notebook.

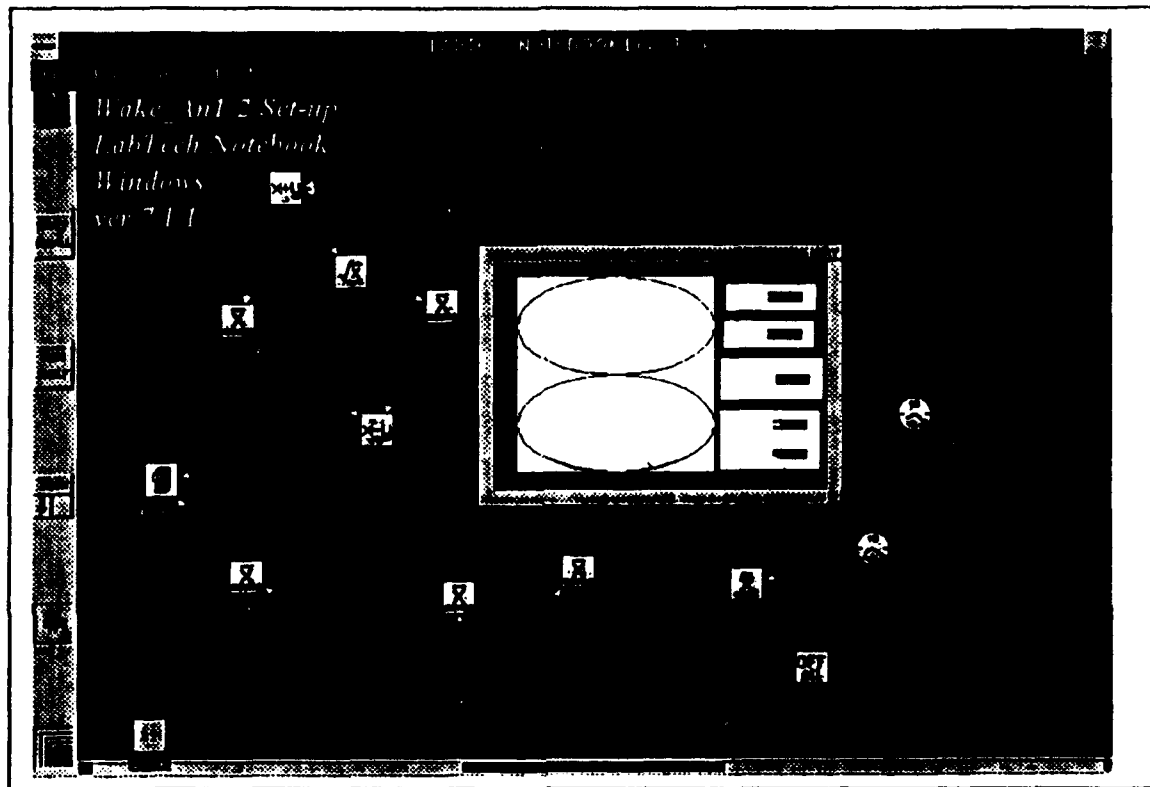


Figure 19. LabTech Notebook Set-Up "WAKE\_AN1/2"

(5) *Expected results.* From the value of maximum expected wake width ( $y'_{wake}$ ) estimated during Run #1 (equation (43)), no appreciable change in pressure should be seen until reaching the interval

$$y_{wake} \text{ (inches)} = 10 \pm \frac{y'_{wake}}{2} \quad (49)$$

Logically,  $q_\infty$  should remain constant during the tunnel run. However,  $q_w$ , the local dynamic pressure in the wake, should change to reflect the condition of the wake as the traverse moves from 0.0 to 20 inches. Also,  $p_w$  should change less than  $(p_0)_w$ . Indeed, many "profile drag" rakes used to measure wake drag from attached flow over airfoils, often have only a single static probe for dozens of total pressure probes [Ref. 4:p. 112]. The static pressure is treated to essentially remain constant through the wake. Actually, due to tunnel wall effects, the static pressure may change slightly [Ref. 1:p. 35]. Nevertheless, it is expected that as the wake is entered,  $q_w$  should get smaller because  $(p_0)_w$  decreases at a faster rate than  $p_w$ .

(6) *Using the data obtained during data acquisition to estimate the drag coefficient.* The software set-up "WAKE\_AN1" in LabTech Notebook is configured to receive the three inputs:  $q_w$ ,  $q_\infty$  and  $y$ . Through a string of "calculation blocks," WAKE\_AN1 forms the plot mentioned earlier of

$$\sqrt{\frac{(p_0)_w - p_w}{(p_0)_\infty - p_\infty}} - \frac{(p_0)_w - p_w}{(p_0)_\infty - p_\infty} \quad v. \quad y \quad (50)$$

which is

$$\sqrt{\frac{q_w}{q_\infty}} - \frac{q_w}{q_\infty} \quad v. \quad y \quad (51)$$

The ordinate of the plot is the integrand from

$$c_d = \frac{1}{r} \int_0^{20} \left( \sqrt{\frac{(p_0)_w - p_w}{(p_0)_\infty - p_\infty}} - \frac{(p_0)_w - p_w}{(p_0)_\infty - p_\infty} \right) dy \quad (52)$$

This equation is integrated from 0.0 to 20.0 inches and the result is an approximation of the drag coefficient. Although the setup WAKE\_AN1 creates a display of the ratios of dynamic pressure versus traverse distance  $y$ , three columns of data are also generated for the student to analyze, using a program such as MATLAB. They are simply the three inputs  $q_w$ ,  $q_\infty$  and  $y$ . It is a simple matter to write a code to use these inputs to solve for  $c_d$ . See Appendix D for an example.

**c. *Run #3 - Wake Analysis Method with Tripped Boundary-Layer***

The only difference between Run #2 and Run #3 is the addition of two "cellophane" adhesive tape strips, 1/2" x 20" x 1 mil. These strips are affixed to the cylinder, approximately 1.25" on either side of the  $\theta$  equals  $0^\circ$  position, parallel to the  $z$ -axis (vertical axis).

The function of these two strips are to act like tiny "vortex generators," which are familiar to all Naval aviators. The strips effectively "trip" the attached boundary layer causing otherwise laminar flow to become turbulent. The consequence of this act is dramatic. By inducing an early transition from laminar to turbulent flow, the engineer can delay actual flow separation, thus delay the formation of the wake. This

in turn decreases the drag produced by an object in an airflow, a favorable situation for blunt bodies [Ref. 2:p. 644].

There is an intuitive explanation for why flow separation is delayed by creating turbulence where there once was laminar flow: In the very small boundary layer, laminar flow can be thought of as flow in 1 dimension only - parallel to the surface. There are no significant forces at work to move the flow either closer toward the surface or farther away. Eventually, however, the displacement of the flow from its original freestream position becomes so great that the laminar boundary layer flow leaves the surface of the airfoil and seeks to return to its former place. If, however, this laminar flow is artificially brought into contact with the surface of the airfoil, which is by no means smooth, the air molecules will be caused to trip and tumble. Specifically, in some random direction in relation to the surface of the airfoil, but in general in a continued downstream direction. As this air trips and tumbles (turbulence) and moves along the surface of the airfoil, it acts like a cartoon snowball rolling down a winter hillside. As it grows, it "reaches" farther above the surface of the airfoil and "gathers" in higher energy air. This higher energy causes the air near the surface to become much faster than it was when it was laminar. This new speed in turn causes the flow to "push" ahead farther along the surface than it naturally wants to go. Eventually the forces at work trying to restore all flows to the original freestream condition overcome the contact between the now turbulent flow and the surface and the airflow separates and is returned to the freestream. Now the point of separation is much farther along and thus the wake width and associated drag is *significantly* reduced.

Anderson, in Reference 2 (p. 643), states:

Because of the agitated motion in a turbulent flow, the higher-energy fluid elements from the outer regions of the flow are pumped close to the surface. Hence, the average flow velocity near a solid surface is larger for a turbulent flow in comparison with laminar flow...because the energy of the fluid elements close to the surface is larger in a turbulent flow, a turbulent flow does not separate from the surface as readily as a laminar flow. If flow over a body is turbulent, it is less likely to separate from the body surface, and if flow separation does occur, the separated region will be smaller. As a result, the pressure drag due to flow separation,  $D_p$  [form drag], will be smaller...

Though not demonstrated in this lab, Hoerner points out in his classic Fluid Dynamic Drag (p. 3-27) yet another way to reduce separation around a stationary cylinder: use suction on the cylinder via a porous surface. This prevents or delays the start of an alternating vortex sheet.

The helicopter industry is already producing aircraft which use a delayed-separation principle called the "Coanda"-effect. The application is NOTAR", which stands for "No-Tail-Rotor" [Ref. 10:p. 1f]. Here blowing, vice suction, is used to manipulate the point of separation around a cylindrical tail boom to provide an asymmetric surface pressure distribution, which then generates desired lift.

## **V. RESULTS**

### **A. ACTUAL CLASS DATA (USING DRAG1.M)**

Table 5 is a summary of the results obtained by using the program drag1.m created in Matlab code, which is located and explained in Appendix D. Users of drag1.m may access the explanation by typing

**> > help drag1**

Drag1.m assumes the following: NPS Low Speed Wind Tunnel and associated TF and calibration factor; tunnel operated at 15 cm H<sub>2</sub>O; equations contained in this thesis are used; data have been edited to remove "idle data."

Table 5 results are from actual classroom data obtained from the three LabTech Notebook set-ups described in Chapter IV. Two AA2801 labs of approximately seven students each were conducted using the upgraded laboratory handout contained in Appendix B. Since this lab was conducted on 9 November 1993, Appendix B has been revised to include the lab times required, Table 1 - Drag Classification, and illustrations under the ZERO/SPAN paragraph.

**TABLE 5. DRAG1.m results**

```
* drag1
% (from data taken during 9 Nov 1993 %
AA2801 Lab)
%
% This data has been reduced using
% DRAG1.m. It has been corrected
% for blockage and is explained in
% APPENDIX D
%
      cdpdu      = 0.71
      cdpd1      = 0.68
      cdpd2      = 0.67
      wakebeg    = 7.3 in
      wakeend    = 12.7 in
      sepaz      = 64.1°
      pft1       = 0.68
      Reeff      = 2.89e+05
      cdwa1      = 0.99
      cdwa2      = 0.18
      percredu   = 81.7 %
```

## **B. PRESSURE DISTRIBUTION METHOD (RUN #1)**

### **1. Data**

Data were obtained, as explained in Appendix B, and filed under PRE\_DIS1.m. Actual results from the classroom are recorded in Appendix C. It should be noted that, in an effort to save space, this DOS Text File has been saved in small print and placed into multiple columns.

The set-up PRE\_DIS1 automatically begins collecting data when the rotator passes  $-17^\circ$  and stops when it passes  $+179^\circ$ . This worked because the rotator itself turned at a constant rate and was controllable electrically. The data were originally saved in two columns:  $\theta$  and  $C_p(\text{raw})$ . All data prior to  $0^\circ$  were manually edited out.

Due to the assumed constant rate of the rotator combined with the constant sampling rate of 10 Hz, the trapezoidal rule was applied to the data using [Ref. 8:p. 193]:

$$A = \left[ \frac{y_{(n)} - y_{(1)}}{2} + \left( \sum_{i=1}^{n-1} y_{(i)} \right) \right] \times \left[ \frac{x_{(n)} - x_{(1)}}{n-1} \right] \quad (53)$$

An uncorrected (for blockage factors)  $c_{dp}$  of 0.71 was obtained using a modified trapezoidal rule:

$$A = \sum_{i=1}^n \left( \frac{y_{(i-1)} - y_{(i)}}{2} \right) \times |x_{(i)} - x_{(i-1)}| \quad (54)$$

Here, equispaced x-values were not assumed.

The blockage factors described earlier (equations (3)-(5)) were applied to the results from both methods, yielding a  $c_{dp}$  of 0.68 using equation (55) and 0.67 using equation (56). Figure 20 shows how the MATLAB program Drag1.m plots  $C_p$  vs.  $\theta$ , and places an asterisk where separation is believed to occur. A routine which assumed  $C_p$  increases abruptly during classical cylinder flow separation predicted the separation azimuth to be  $64.1^\circ$ . This value for theta was then used with equations (43) and (51) to estimate the wake width, which ranged from 7.3 to 12.7 inches.

Next, Matlab-defined functions "polyfit" and "polyval" were used to generate a fifth-order polynomial approximation to the actual data. In this case, a fifth-order polynomial was chosen as it best fit the plot given. Results are shown in Figure 21.



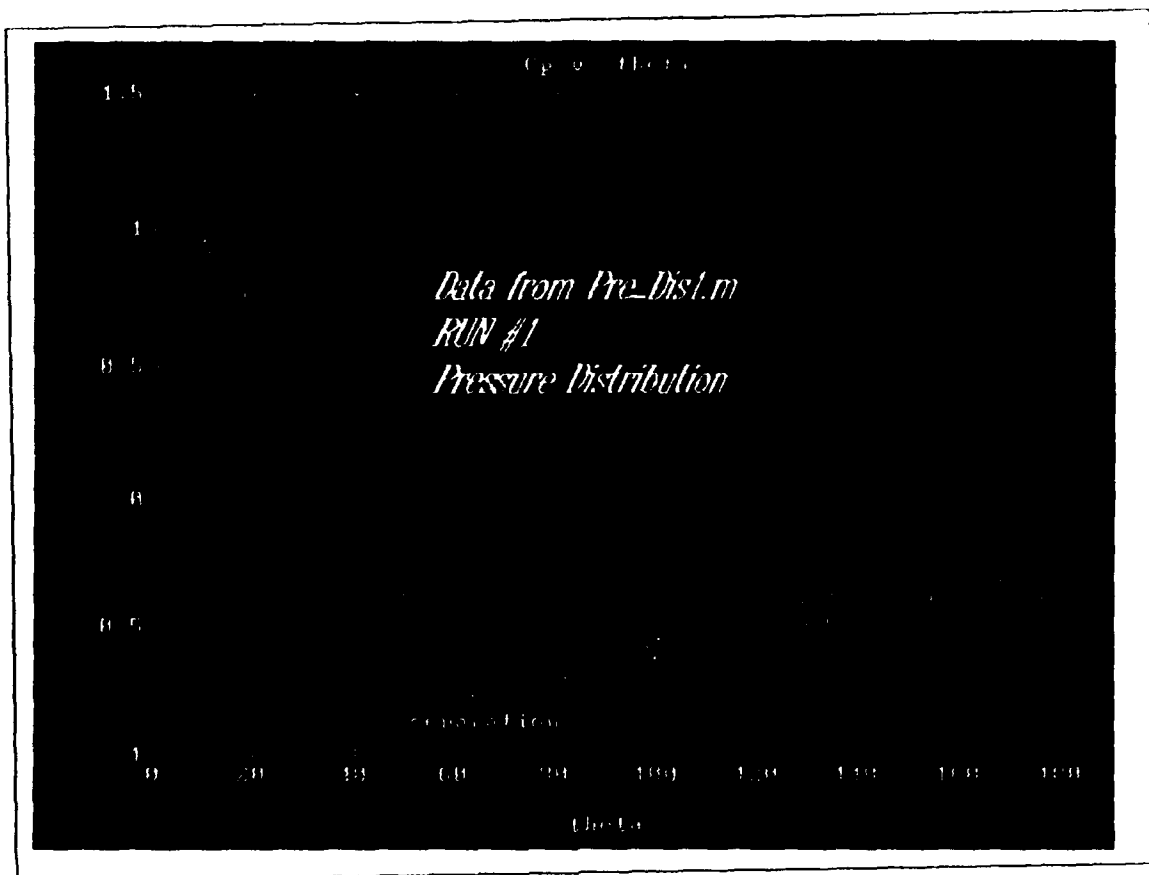


**Figure 20.** The Separation Point Estimated by SEPAZ

Finally, the effective Reynolds number of  $2.89 \times 10^5$  was calculated using equations (7), (8), (13) and (46).

## 2. Analysis

The corrected  $c_{dp}$ 's plot close to but not on the empirical data shown in Figure 24. One reason why 0.67 is seemingly low is that the pressure distribution method does not measure  $c_d$ ; it only measures the component due to pressure (form drag). In fact, Panton, in Incompressible Flow [Ref. 9:p. 386], was responsible

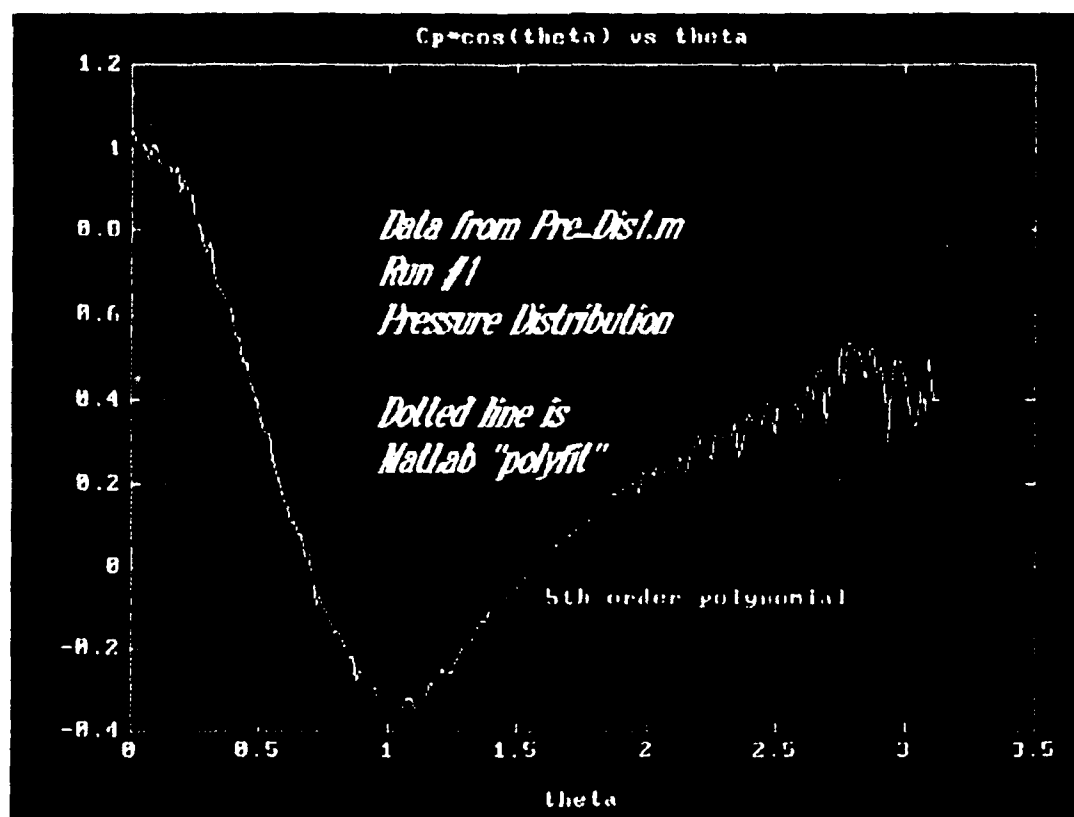


Figure 21-7. Comparison of Matlab polyfit with the data.

Using the data in Figure 24 from the different sources, H. H. Hesterman et al. [19] have fitted the data to a 5th order polynomial. What they have done is to take the data from Figure 24 and fit it to a 5th order polynomial. The result is shown in Figure 25. The data is shown as a dotted line and the 5th order polynomial is shown as a solid line. The data is from the same sources as in Figure 24. The 5th order polynomial is a good fit to the data. The data is shown as a dotted line and the 5th order polynomial is shown as a solid line. The data is from the same sources as in Figure 24. The 5th order polynomial is a good fit to the data.

### C. WAKE ANALYSIS METHOD (RUNS #2,3)

#### 1. Data

Essentially the same methods just explained were used to find  $c_d$  related to the wake analysis from Chapter V, Section B. Equation (56) was used to find  $c_d$  for Run #2 (0.99) and Run #3 (0.18). The wake analysis method uses the WAKE\_ANI/2 set-ups and from data reduction using DRAG1.m, the following plots were generated (Figures 22 and 23):

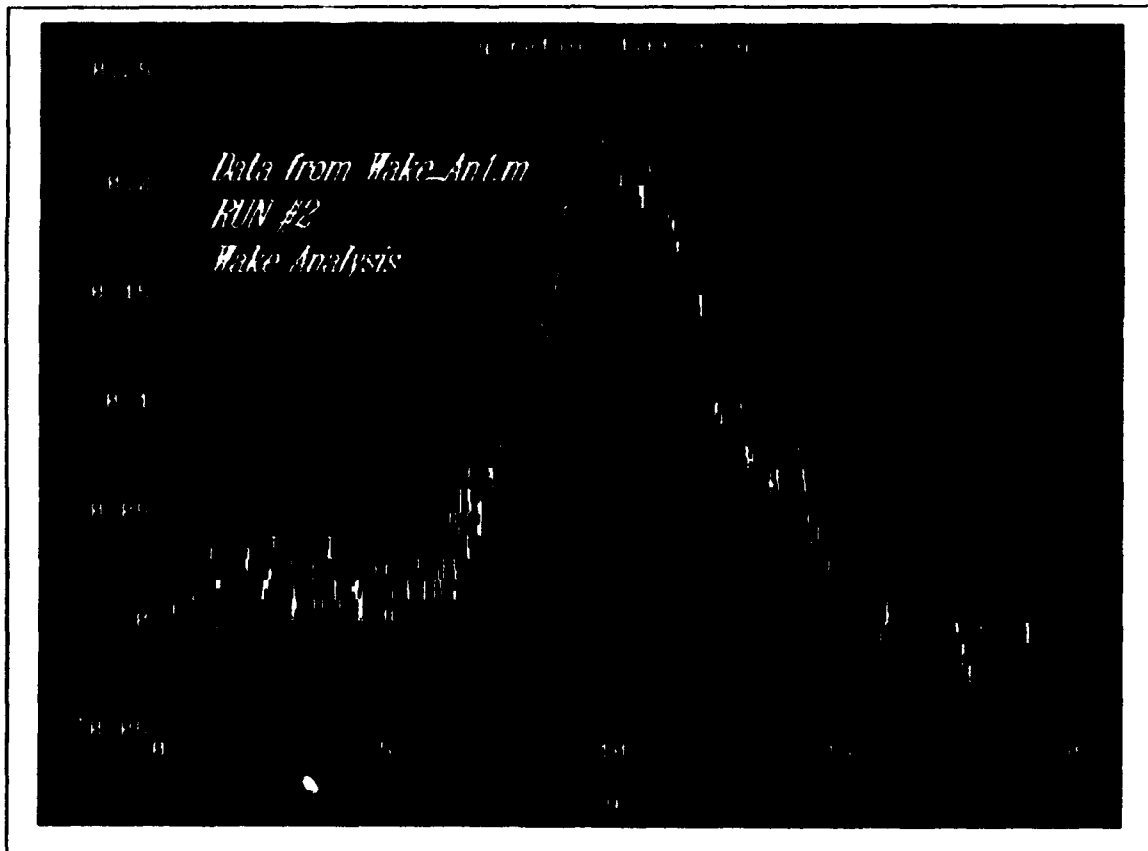


Figure 22. WAKE\_ANI Results (Run #2)

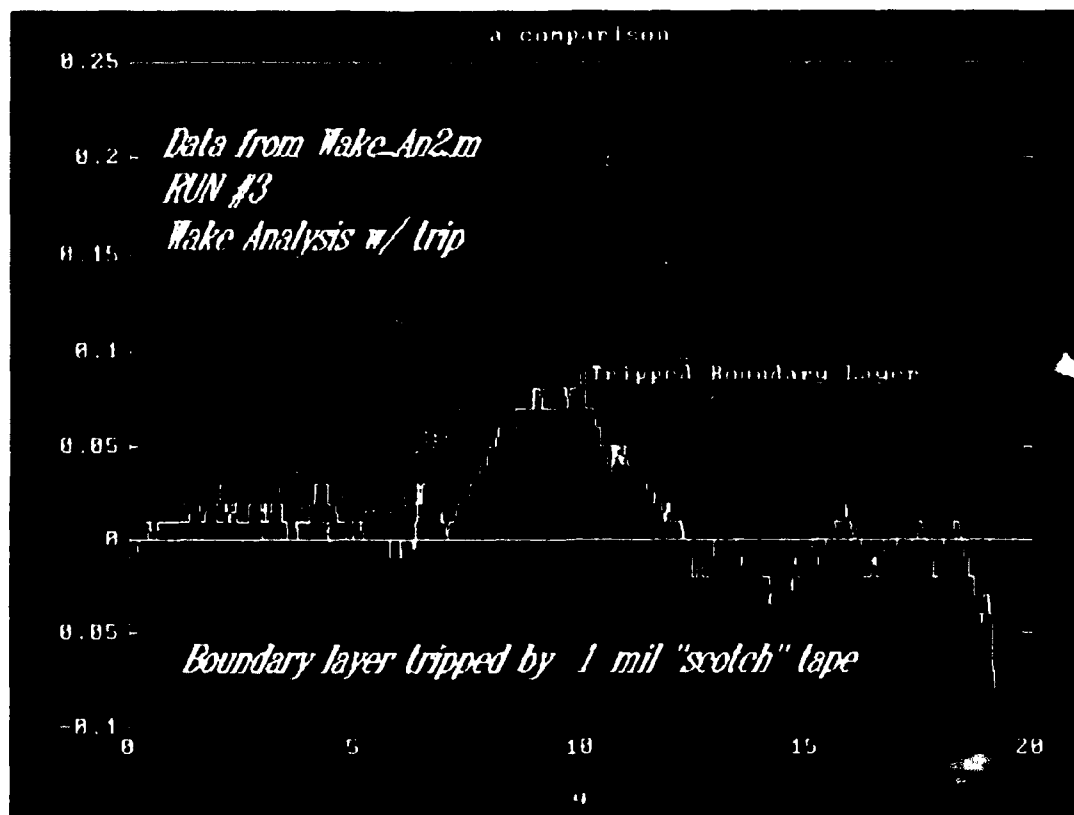


Figure 23 WAKE-AN2 Results Compared (Run #3)

To use these data (also recorded in Appendix C), the "idle points" were first edited out. Unlike the first set up during which the sampling rate was a steady 10 Hz, the movement of the pitot static probes on the traverse was entirely dependent on the speed and accelerations of the student doing the cranking. Additionally, no provision was made to automatically start or stop the data acquisition. A keypress initiated the data collection and selecting EXIT stopped it. Consequently, idle data existed on both ends

of the data files. These idle data were easy to detect. All data prior to the  $y$ -value ( $\theta$ ) increases and all data after it stops increasing were edited out.

Figure 24 shows the results of all three runs plotted against empirical data.

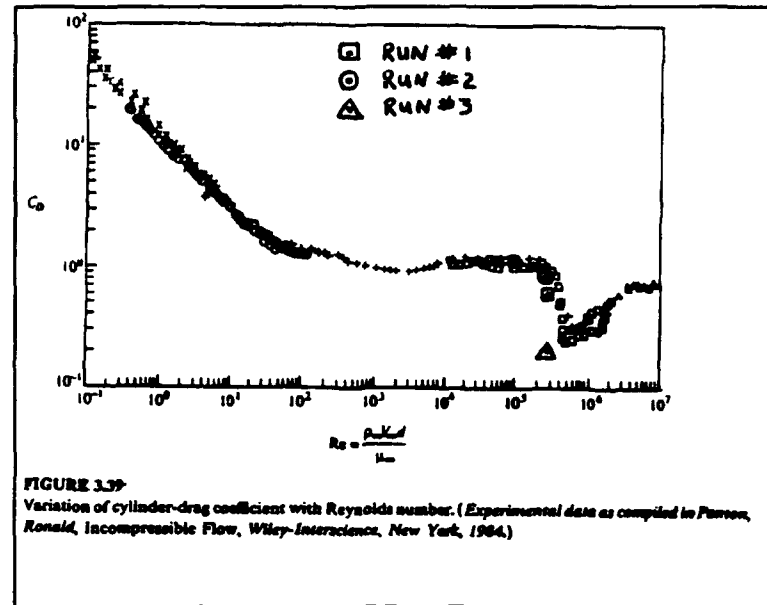


Figure 24. Results Plotted Against Empirical Data

## 2. Analysis

Again, the corrected  $c_d$  from Run #2 was plotted against the  $Re_{eff}$  and compared to the empirical data. It compared very favorably, tending to validate the TF given. Also, from Figure 22, the wake analysis width prediction of DRAG1.m seemed reasonable.

The 81.7% reduction in  $c_d$  from Run #3 is dramatic. If this number is high, then the TF might come into question again. "The higher the freestream turbulence, the more readily transition takes place [Ref 2:p. 389]." Golf balls use dimples to accomplish similar levels of dramatic drag reduction.

There is one concern that arises out of Figures 22 and 23. It would appear that given the use of equation (53) it should be quite impossible to ever have a negative solution, as was seen during both runs. There are two possible explanations for this phenomenon: (1) As shown in Figure 25 and as discussed on page 35 of Reference 1, it is theoretically possible to have  $q_w$  become larger than  $q_\infty$ . Were this to happen, the plot of equation (53) would indeed be negative for that interval. (2) A more likely reason, though, is that the signal from the  $q_w$  or  $q_\infty$  transducer is either poorly scaled or actually drifts with either time or with displacement. This could be easily verified by repeating a traverse of the test section in both directions, with the cylinder removed, and comparing  $q_w$  to  $q_\infty$ . Unfortunately, time did not allow for this verification and a solution to the negative values seen in Figures 22 and 23 are left for future exploration. For this thesis, the data were neither adjusted up nor down (from the zero axis), nor was the plot in Figure 22 pivoted by anchoring the left end and rotating the right end of the plot up to the zero axis. These corrective methods might result in a better approximation, but it remains to be seen whether data acquisition or tunnel velocity profiles are responsible for the negative values.

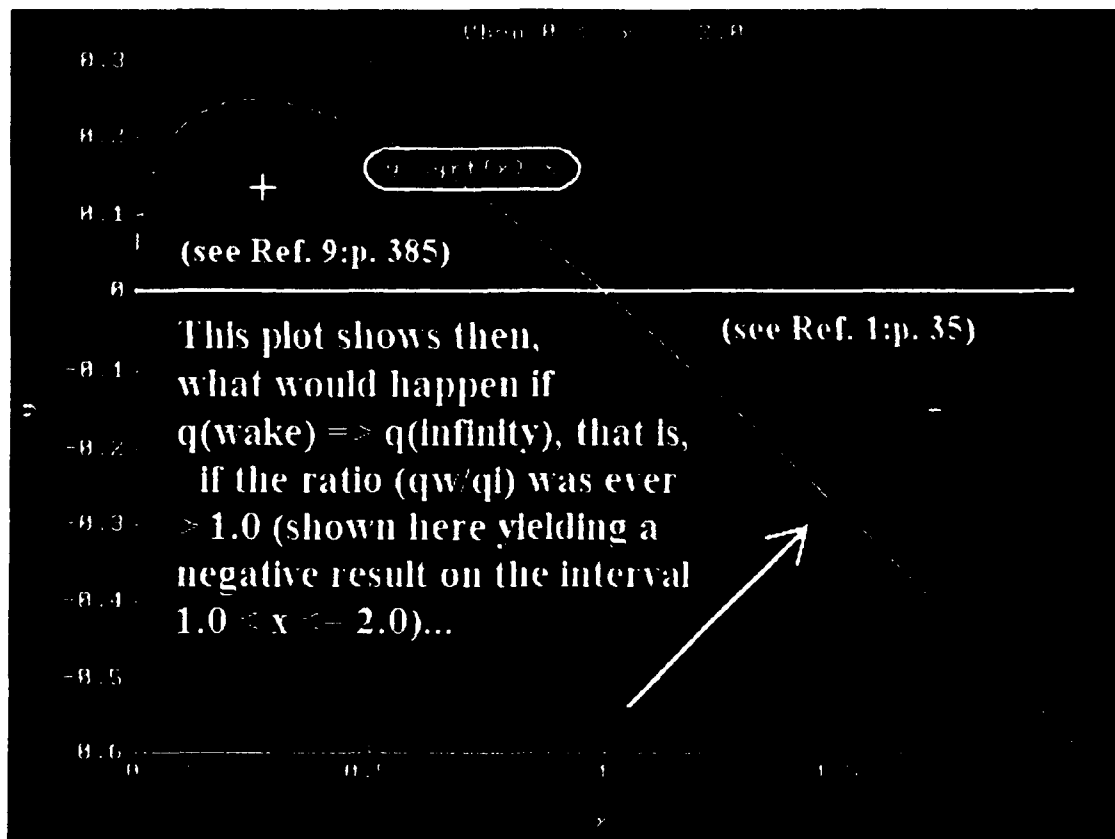


Figure 25. Graph of the Equation  $y = \sqrt{x} \cdot x$

## VI. CONCLUSIONS

### A. UPGRADE LIMITATIONS

#### 1. Wake Analysis Method

Rae and Pope point out in Reference 4 (pp. 214-217), that the wake analysis method has several "gray areas:"

1. How do you measure spanwise variation of the profile drag behind an airfoil? [p. 213]
2. Are vortices present at higher Re? [p. 214]

3. Is true two-dimensional flow a function of  $Re$  or does it really exist? [p. 214]

The authors state twice:

It is well known that the wake survey is not valid...where separation is present...cannot measure momentum loss caused by separation or fluid rotation. [p. 214,217]

The limitations, then, are that it is yet unknown exactly how valid the approximation of  $c_d$  is from the wake analysis method. Certainly flow separation *is* present. While the value obtained,  $c_d = 0.99$ , fits that empirical data, enough questions are raised by Rae and Pope that no strong conclusions may be drawn at this time.

## 2. Hardware

Current hardware returns signals on the order of  $10^{-3}$  volts. Subsequent amplification of these tiny signals has the effect of amplifying noise or simply limiting the usefulness of the signal. The Analog-to-Digital data acquisition card used in this lab has the ability to resolve signals down to 4095 parts. In some cases, the only signals possible were confined to a range of 0.000 to 0.009 volts (see Table 3, Appendix B). Meanwhile, the smallest range LabTech Notebook can program down to read is  $\pm 0.625$  volts. This means that

$$\frac{+0.625 - (-0.625) \text{ volts}}{(4096 - 1) \text{ counts}} = \pm 0.00033 \frac{\text{volts}}{\text{count}} \text{ resolution} \quad (55)$$

Dividing an actual useful range of 0.009 volts by this resolution yields an approximate effective resolution down to just 28 signals discriminating between 0.000 and 0.009 volts.



Put another way, while the A/D card can resolve down to 4095 parts, only 28 of these parts are being used, less than 1 % of the card's capability.

### **3. LabTech Notebook**

This software application requires considerable time to learn. Having a qualified user available helps greatly. The lengthy tutorial, once mastered, provides an excellent foundation for using this software package to do data acquisition.

Beyond the time it took to learn, it has three other limitations:

1. apparent limited sampling rate of 1000 Hz
2. very limited graphics capability
3. high memory usage in the Windows environment.

## **B. RECOMMENDATIONS**

### **1. Study the Wake Analysis Method Further**

A survey of the static pressure in the wake behind the cylinder should be taken and compared to the freestream static pressure. If the static pressures vary significantly, the cylinder should be replaced and the tunnel velocity profile measured along the traverse, paying close attention to the ends. The velocity along the traverse should be checked for speeds which are greater than freestream. Rae and Pope warn that  $q$  must be taken as far behind the cylinder so that  $p_w$  equals  $p_\infty$  [Ref. 4:p. 216]. If the wake velocity remains less than the freestream velocity, check for signal noise or other faulty modes of the data acquisition system.

## **2. Match Hardware to Software Capability**

The 12-bit resolution of the A/D card as just explained, combined with as large an output as possible, would yield a higher resolution than currently available. This means that the signals into the PC should have as wide a range as possible, not the current 9 millivolt range output currently seen. This output is both a function of the signal transducer and potentiometer and signal conditioner. If the hardware used to acquire signal sources must remain, then the signal conditioner must be reconfigured to amplify the output. If the sources can be measured using devices which discriminate well below .033 millivolts level, then the signal conditioners need not be changed.

## **3. Investigate Better Data Acquisition Software**

Investigate non-Windows applications for better response to memory limitations of PC. Also, recommend obtaining, for long-time use, a data acquisition program which has a broader graphics package than LabTech Notebook currently employs.

## **4. Validate TF**

Since no attempt was made to validate the turbulence factor, the TF should be recalibrated using procedures discussed in Reference 1. TF is important and contributes approximately equally with the blockage factors in the calculation of the effective Reynolds number (equation (8)).

## **5. Upgrade the NPS Low Speed Wind Tunnel deck**

The next logical step in the wind tunnel upgrade is to match the data acquisition capability with the actual layout of the tunnel test facilities. Layers of old thesis projects, built upon each other over the years, can effectively be replaced with this data acquisition system. Former procedures and techniques may be incorporated into the

set-ups in LabTech Notebook on an as-needed basis. Furthermore, the current collection of signal conditioners, signal amplifiers, multiplexer and wiring inhibits easy access to the test section. The PC used in this thesis must be located a full twenty feet away from the test section making lab observation and display observation all but exclusive events. A permanent wood lab table extending from the test section along the diffuser, would be a practical way to provide this easy access and give a place for lab equipment, in component form, to be set up. Furthermore, a system of annually justifying the continued presence of former thesis projects is required to prevent the problem of layering. Copies of thesis reports should be readily available near each project left intact after the author, student or professor, transfers from the school.

## APPENDIX A: PREVIOUS LAB HANDOUT

### Drag on a Cylinder

#### Objectives

The drag on a circular cylinder which spans the height of the wind tunnel test section will be determined using wake analysis and pressure distribution methods, demonstrating basic wind tunnel methodology, including operating procedures, Reynolds number calculation and application of wind tunnel correction factors.

#### Apparatus

The NPS low speed wind tunnel is described in detail in the NPS Laboratory Manual for Low Speed Wind Tunnel Testing. A circular cylinder (length = 28.0 in., diameter = 2.96 in., volume = 192.68 in<sup>3</sup>) is placed in the wind tunnel such that it spans the test section height. A single static port is built into the mid-portion of the cylinder. The cylinder itself, is attached to an electrically operated rotatable base. In the aft portion of the test section are placed two pitot-static probes, aligned such that one provides total pressure and the other static pressure, in the same longitudinal plane. These probes are attached to a traverse mechanism which enables lateral positioning (across the width of the test section) to be varied. Pitot-static pressures are transduced by strain gauges and output voltages fed to x-y plotters (y-information). Additionally, sensors on both the rotatable base and traverse mechanism provide position signals to the plotters (x-information). Thus, wind tunnel output consists of five electrical signals:

$$P_{wake} = P_2$$

$$q_{wake} = q_2$$

$$P_{cylinder} = P_\theta$$

Cylinder position ( $\theta$ )

Probe location

The tunnel will be run at a pressure differential of 15 cm  $H_2O$  (approximately 115 kts.)

## Wake Analysis Methodology

Applying the Reynold's [sic] Transport Theorem to Newton's Second Law,

$$\Sigma F = \frac{\delta}{\delta t} (\text{momentum})$$

and writing the resultant equation for a control volume (see Zucker: Fundamentals of Gas Dynamics, p. 65-69) results in:

$$C_d = \frac{2}{d} \int \left[ \frac{V_2}{V_1} - \left( \frac{V_2}{V_1} \right)^2 \right] \delta y - \frac{1}{d} \int \left[ \frac{P_2 - P_1}{q_1} \right] \delta y \quad (4.1)$$

## Pressure Distribution Methodology

The forces on a cylinder may be modeled as shown in Figure 21.

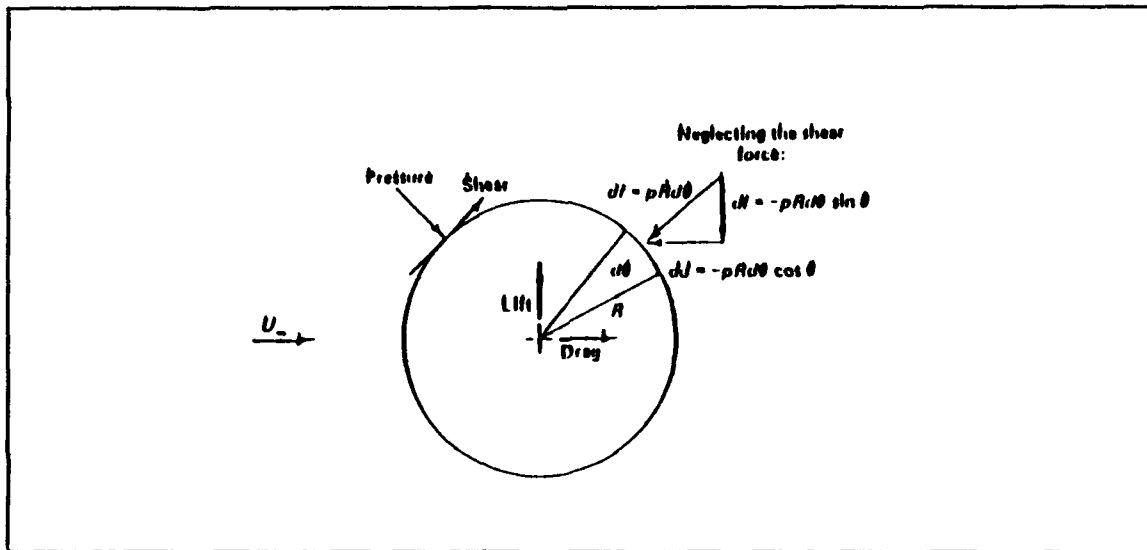


Figure 21. Aerodynamic Forces on a Cylinder

Below the critical Reynold's [sic] number, the form drag is the dominant component of the resultant force on the cylinder. (Typically, total parasite drag is composed of approximately 80% form drag and 20% skin friction drag.) For blunt bodies (see Bertin and Smith: Aerodynamics for Engineers, p. 88-91), form drag can be approximated by the expression:

$$C_d = \int_0^\pi C_p \cos \theta \delta \theta$$

$$C_d = \int_0^\pi \frac{P_\theta - P_1}{q_1} \cos \theta \delta \theta \quad (4.2)$$

### X-Y Plotter Calibration

X-Y plotters can be calibrated to provide the following ratios:

$$\frac{q_2}{q_1} = (V_2/V_1)^2 \text{ vs. } y$$

$$\frac{P_2 - P_1}{q_1} \text{ vs. } y$$

$$\frac{P_\theta - P_1}{q_1} \text{ vs. } \theta$$

From the curves of these ratios, the integrals of equations (4.1) and (4.2) may be evaluated. Calibration of the plotters is accomplished as follows:

•  $(V_2/V_1)^2$  vs.  $y$ :

1. The plotter pen is positioned at the zero point prior to starting the tunnel ( $V_2 = 0$ ).
2. After the tunnel is at full speed, with probes located away from the wake ( $V_2 = V_1$ ), the plotter pen is positioned at the  $(V_2/V_1)^2 = 1.0$ ,  $y=0$  point.
3. The probes are then traversed across the test section (20 in.) and appropriate ratios are plotted.

$$\bullet \frac{P_2 - P_1}{q_1} \text{ vs. } y:$$

1. After the tunnel is at full speed, with probes located away from the wake ( $P_2 = P_1$ ), the plotter pen is positioned at the  $C_p = 0.0$ ,  $y=0$  point.
2. The probes are traversed across the test section and the appropriate ratios versus  $y$  are plotted simultaneously.

$$\bullet \frac{P_\theta - P_1}{q_1} \text{ vs. } \theta:$$

1. The plotter pen is positioned at the  $C_p = 0$  point prior to starting the tunnel.
2. With the tunnel running, the cylinder is rotated such that  $\theta = 0^\circ$ , which puts the static port at the stagnation point ( $P_2 = P_1 + q_1$ , and the ratio equals unity). The plotter pen is positioned at the  $C_p = 1.0$ ,  $\theta = 0^\circ$  point.
3. The cylinder is rotated to the  $\theta = -20^\circ$  position and plotting begins (from  $\theta = -20^\circ$  to  $180^\circ$ ).

## Laboratory Procedures

1. Determine atmospheric pressure:

$$P_{atm} = (\text{baro. reading}) + (\text{temp corr.}) + (\text{lat. corr.})$$

(Latitude correction = -.0245)

2. Determine temperature.
3. Make required wind tunnel runs.
4. Trip the boundary layer and make an additional run in order to determine the reduction in wake size afforded by a turbulent boundary layer. (Wake analysis methodology only.)

## Conversions and Constants

$$\mu_{air} = 3.8 \times 10^{-2} \text{ lbf}\cdot\text{s}/\text{ft}^2$$

$$R_{air} = 53.3 \text{ ft}\cdot\text{lbf}/\text{lbm}\cdot^\circ\text{R}$$

$$^\circ\text{R} = ^\circ\text{F} + 460$$

$$1 \text{ cm H}_2\text{O} = 2.045 \text{ psf}$$

$$1 \text{ psi} = 2.036 \text{ in Hg}$$

$$q = \Delta P / .93 \text{ (Calibration factor)}$$

## Report Requirements

1. Calculate the effective Reynold's [sic] number and determine the corresponding empirical drag coefficient from Figure 22.
2. Utilizing x-y plotter curves, evaluate the integrals of equations (4.1) and (4.2) and determine experimental drag coefficients for each method, applying wake and solid blockage correction factors.
3. Determine the percentage reduction in drag afforded by a turbulent boundary layer.
4. Briefly discuss results.

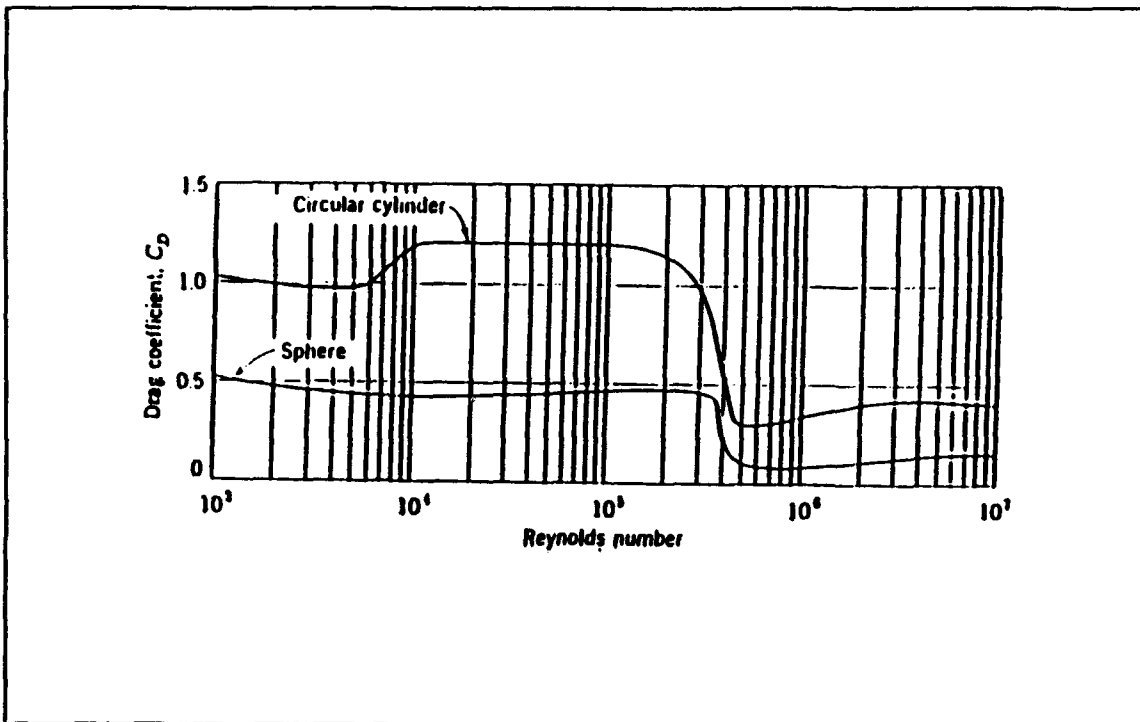


Figure 22. Cylinder Drag Coefficient



## APPENDIX B: UPGRADED LAB HANDOUT

### CYLINDER DRAG EXPERIMENT

Class time: :50  
Lab time: 1:30  
Report time: 3:00  
Total time: 5:20

#### \*\*\*Before the Lab\*\*\*

You will need to read this handout as well as pages 11-15, 32-38 of the NPS Laboratory Manual for Low Speed Wind Tunnel Testing. You will also need to bring either 3½" or 5¼" formatted floppy disk with at least 100 KB space available.

#### Objectives

A current method of PC-based automated data acquisition using a combination of pressure transducers, potentiometers, signal conditioners and amplifiers will be used to collect and analyze data from flow over a non-rotating cylinder. Two techniques of drag determination (pressure distribution and wake analysis) will be used, demonstrating basic wind-tunnel methodology. In addition to these two primary objectives, students will be introduced to the NPS low speed wind tunnel operating procedures to include tunnel calibration and tunnel correction factor.

#### Apparatus

The NPS low speed wind tunnel is described in detail in the NPS Laboratory Manual for Low Speed Wind Tunnel Testing. Figure 21 shows the signal path for the data acquisition system. The dimensions of the cylinder are  $d=2.96$  inches,  $h=28.4$  inches. The dimensions of the test section are  $w=45.0$  inches,  $h(\text{above reflection plate})=28.4$  inches. There is a single pressure port near the center of the cylinder. The cylinder is mounted to an electrically rotatable base which is able to rotate from  $-20$  degrees to  $+180$  degrees in a clockwise fashion. Behind the cylinder, on a manual traverse, is a combination pitot-static probe apparatus. The probes may be moved along the traverse in the  $y$ -direction from 0 to  $+20$  inches. The transducers, potentiometers, signal conditioners and amplifier which connect these measuring devices to the data acquisition card inside the PC are shown in Figure 21. Specific information about each device is located in Table 1. The wind tunnel will be run in 4th gear at  $15 \text{ cm H}_2\text{O } \Delta p$ . This

" $\Delta p$ " is a 15 cm  $H_2O$  difference between the local static pressure entering the contraction cone ( $p_1$ ) and the local static pressure leaving the contraction cone and entering the test section ( $p_2$ ). Previous wind tunnel calibrations have experimentally shown this particular difference of 15 cm  $H_2O$  to equate to approximately 115 MPH.

In general, the calibrated NPS low speed academic wind tunnel equation is

$$\Delta p = 0.243 (cm H_2O) + 0.895 q_{test\ section} \quad (1)$$

Dynamic pressure is

$$q_{test\ section} \approx q_{\infty} = \frac{1}{2} \rho_{\infty} V_{\infty}^2 \quad (2)$$

where

$$\Delta p \left( \frac{lb}{ft^2} \right) = [p_1 - p_2](cm) [\gamma_{water}] \left( \frac{lb}{ft^3} \right) \left[ \frac{1\ ft}{30.5\ cm} \right] \quad (3)$$

and

$$\gamma_{water} \approx 62.35 \frac{lb}{ft^3} \quad (4)$$

Combining equations (1) through (4) and taking density in slugs/ $ft^3$ ,

$$\therefore V_{\infty} \left( \frac{ft}{sec} \right) = \sqrt{\frac{2(\Delta p - 0.243)}{0.895 \rho_{\infty}}} \quad (5)$$

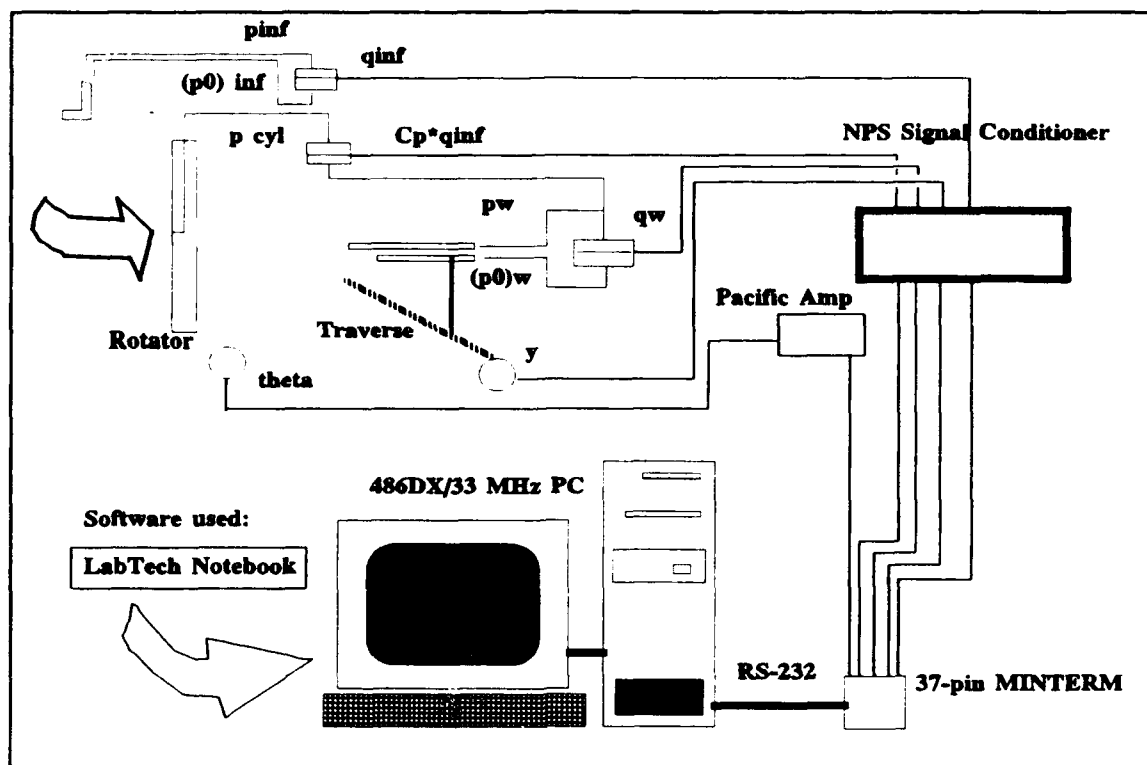


Figure 21. Signal Path of Data Acquisition System

## Terminology

$p_0$  = total (stagnation) pressure  
 $p$  = static pressure  
 $q$  = dynamic pressure =  $p_0 - p$

$(p_0)_\infty$  = freestream total pressure (associated with freestream velocity)  
 $p_\infty$  = freestream static pressure (associated with freestream velocity)  
 $q_\infty$  = freestream dynamic pressure =  $(p_0)_\infty - p_\infty$

$(p_0)_w$  = wake pressure measured behind the cylinder at the probe  
 ( $(p_0)_w$  assumed to =  $(p_0)_\infty$  when taken outside wake)  
 $p_w$  = static pressure measured behind the cylinder at the probe  
 ( $p_w$  assumed to =  $p_\infty$  when taken outside wake)

$q_w$  = wake dynamic pressure =  $(p_0)_w - p_w$   
 $p_{cyl}$  = pressure measured at the cylinder  
 $D_p$  = Form Drag (due to separated flow)  
 $D_f$  = Shear Drag (due to skin friction)  
 $C_p$  = pressure coefficient  
 $c_{du}$  = uncorrected drag coefficient  
 $c_d$  = drag coefficient relating to total drag or profile drag  
 $c_{dp}$  = drag coefficient due to  $D_p$  only  
 $r$  = radius of cylinder  
 $\theta$  = azimuth of the rotator (signal from potentiometer)  
 $y$  = position of the traverse (signal from potentiometer)

### Conversion Constants

latitude correction = -0.0245 in. Hg

temperature correction = (see Table 4-2 on bulletin board near tunnel)

$\mu_{air} = 3.8 \times 10^{-7}$  (lbf-s)/ft<sup>2</sup>

$R_{air} = 53.3$  (ft-lbf)/(lbm-°R)

°R = °F + 460

1 ft = 30.48 cm

1 cm H<sub>2</sub>O = 0.0142 psi

1 psi = 2.036 inches Hg

$q_{test\ section} = (\Delta p - 0.243)/.895$  (NPS wind tunnel calibration equation)

TF = 1.04 (NPS wind tunnel turbulence factor)

TABLE 1. Drag Classification

TOTAL DRAG - D		
SHEAR - $D_f$ (due to skin friction)  Dominates streamlined bodies	NORMAL (due to pressure)	
	Form - $D_p$ (due to separation)  Dominates blunt bodies	Induced (due to lift)
	Profile Drag = $D_f + D_p$ (2-D)	
Parasite Drag = $D_f + D_p$ (3-D)		

### Pressure Distribution Method

For blunt objects in subsonic airspeeds, form drag dominates the resultant force on a non-rotating cylinder in airflow. The pressure distribution method only measures  $D_p$ . Using Bertin and Smith's Aerodynamics for Engineers, p. 60 or Anderson's Fundamentals of Aerodynamics, p. 209:

$$c_{d_p} = \int_0^\pi \frac{p - p_\infty}{q_\infty} \cos\theta \, \delta\theta, \text{ where } C_p = \frac{p - p_\infty}{q_\infty} \quad (6)$$

### Wake Analysis Method

Comparatively, the wake analysis method measures not force, but a change in velocity. It is a ratio of dynamic pressures, which reduce to a ratio of velocities according to equation (2). The wake analysis method accounts for profile drag, or  $D_f + D_p$ . From Rae & Pope's Low-Speed Wind Tunnel Testing, p. 215:

$$c_d = \frac{1}{r} \int_0^{20} \left( \sqrt{\frac{(p_0)_w - p_w}{(p_0)_\infty - p_\infty}} - \frac{(p_0)_w - p_w}{(p_0)_\infty - p_\infty} \right) dy \quad (7)$$

### Data Acquisition

The heart of any PC-based data acquisition system is the data acquisition A/D (Analog/Digital) board. This device takes analog signals such as voltages and converts them to digital signals for the computer software to use. In the case of this laboratory, pressure signals and position signals, in the form of output voltages (Vdc) are first conditioned for optimum signal gain, then channeled to the A/D board via a standard RS-232 terminal. The A/D board simply plugs into the inside of the PC and has two settings which are of interest to the user:

1. 8/16 Channel Select - 8-channel differential input (normal or floating) or 16-channel single-ended input. This lab uses 8-channel floating differential input (Channels 0-7). The term "floating" merely refers to the method of providing a common ground to eliminate unnecessary noise.

2. **Gain/Range** - manual or programmable. The A/D board used in this lab has a programmable gain/range accessible through the software. The gain/range may be set differently for each input device and for all uses of that input device. Bipolar and unipolar refer to the polarity of the range. An example of bipolar gain/range would be  $\pm 5V$ . Unipolar might be 0-5V.

Once the signals have been properly fed into the A/D board it's up to the software to use the signals to provide actual data acquisition. This includes accepting the data, displaying the data and storing the data. Data that have been stored (for example a file of two columns of data: elapsed time and temperature) may then be retrieved into a spreadsheet and plotting program (such as Lotus 1-2-3<sup>®</sup>) or into a math processor (such as MATLAB<sup>®</sup>) to be analyzed. The convenience of the PC allows the operator to do this at one place and at essentially one time.

A typical method of calling a data file into MATLAB<sup>®</sup>, for instance, would be:

```
>> load A:\pre_dis1.m
>> whos % will display size of matrix [m,n] (you will need m)
>> x=pre_dis1(1:m,1); % creates a column vector x of the first column of data in pre_dis1
>> y=pre_dis1(1:m,2); % creates a column vector y of the second column of data in pre_dis1
>> plot(x,y),grid % creates a plot of x vs. y
```

In this AA2801 lab, the following data will be generated by LabTech Notebook:

**TABLE 2. File Organization**

	Column 1	Column 2	Column 3
<b>Pre_Dis1.m</b>	$\theta$	Cp (Raw)	Cp (theoretical)
<b>Wake_An1.m</b>	y	$\sqrt{\frac{q_w}{q_\infty}} - \frac{q_w}{q_\infty}$	
<b>Wake_An2.m</b>	y	$\sqrt{\frac{q_w}{q_\infty}} - \frac{q_w}{q_\infty}$	

If the A/D board is the "heart" of data acquisition then the software is the "brains." Data acquisition software programs (such as LabTech Notebook<sup>®</sup>) allow the operator to configure "set-ups" which tell the PC how to collect, display and store the data. Current software uses block icons which may be cascaded into an infinite number of combinations of configurations.

## Safety Procedures

Prior to executing the lab, normal pre-operating safety checks should be made. Students should use proper hearing protection for tunnel speeds above 5 cm H<sub>2</sub>O.

## Initial Procedures Prior to Running the Tunnel

1. Determine atmospheric pressure ( $p_{\text{atm}} = (\text{baro}) + (\text{temp. corr.}) + (\text{lat. corr.})$ )  
 $p_{\text{baro}} = \underline{\hspace{2cm}} \quad p_{\text{atm}} = \underline{\hspace{2cm}}$
2. Observe tunnel temperature...  $T_{\text{atm}} = \underline{\hspace{2cm}}$
3. Ensure the following prior to tunnel runs:
  - a. Top rack signal conditioners - ON (switch/light is on)

### Caution

Do not change or attempt to adjust any settings at this time

- b. Traverse is in  $y = 0.00$ " position (visual inspection)
  - c. Rotator is in  $\theta = 0^\circ$  position, toggle switch = RUN, speed control = 75 (visual inspection)
  - d. 486DX/33MHz PC turned ON and in Windows Program Manager
  - e. HP Laser Jet II Plus turned ON with paper loaded
  - f. Double doors and door to room H-033A CLOSED
4. Double-click "Build-Time" under the "Wind Tunnel" menu (you are now in LabTech Notebook's ICONview - you may need to click the uppermost right button to stretch the window so that you can see the entire set-up)

Note: Because of the memory usage involved, waiting for WINDOWS to complete each input before assigning another will reduce the potential to overload the PC; if the PC is overloaded, chances are you will have to reset and start over.

## **5. Perform ZERO and SPAN**

### **Calibration**

The lab technician will ensure the data acquisition lab has the proper initial settings and that the input devices are properly calibrated. The configuration outputs should be "scaled" at this time using the set-up "ZERO" and "SPAN."



**TABLE 3. AA2801 Cylinder Lab Initial\* Settings**

Channel	0	1	2	3	4
Run	1	2,3	2,3	1	2,3
Signal	$P_{cyl}-P_{\infty}$	$(P_0)_w-P_w$	$y$	$\theta$	$(P_0)_{\infty}-P_{\infty}$
HI	37	36	35	34	33
LO	18	17	16	15	14
LLGND	19	28	29	15 -J- > 29	19
Sig. Cond.	#2	#1	#3	Pac. #2	#10
Amp?	No	No	No	Pac. #2, x100	No
Zero pt.	0 cm	0 cm	$y=0''$	$\theta=-18^{\circ}$	0 cm
*Zero (v)	0.00v	0.00v	0.00v	-0.18v	0.00v
Span pt.	15 cm, $\theta=0^{\circ}$ , $y=0''$	15 cm, $y=0''$	$y=20''$	$\theta=+180^{\circ}$	15 cm
*Span (v)	0.009v	0.0054v	.0200v	1.80v	0.009v
Scale Factor	x110	x185	x1000 + 2.0	x100	x110
Polarity	Bipolar	Bipolar	Bipolar	Bipolar	Bipolar
Gain	$\pm 0.625v$	$\pm 0.625v$	$\pm 0.625v$	$\pm 2.50v$	$\pm 0.625v$
<p align="center">"12 Bit Resolution"  <math>(2^{12} = 4096 \text{ divisions available})</math></p> <p align="center">example:</p> $\frac{+1.25 - (-1.25) \text{ volts}}{(4096 - 1)} = \pm 0.305 \text{ mV resolution}$					

"Table 3 show "initial settings" only and is intended for the technician to use prior to the beginning of the AA2801 Cylinder Lab. LabTech Notebook (LTNB) setups "ZERO," "SPAN" and accompanying directions should be used for *final* settings.

## Using "ZERO" and "SPAN"

All input devices are referenced to some zero and to some secondary value, which yields a "span." That is, some mode of their output where the user wants 0.00 volts and some other voltage as a return. Everything is considered linear after the zero and span are set to a desired output. Normally a Digital Volt Meter (DVM) is used to verify such an output. However, for automatic data acquisition, it's more important to verify the output at the PC since the data are being collected here. (It is possible for noise to affect what is read after the signal conditioner so that the signal has changed by the time it is displayed on the monitor.) The "ZERO" and "SPAN" set-ups were designed to give the user a visual display of his/her zero and span for each device used in the cylinder lab.

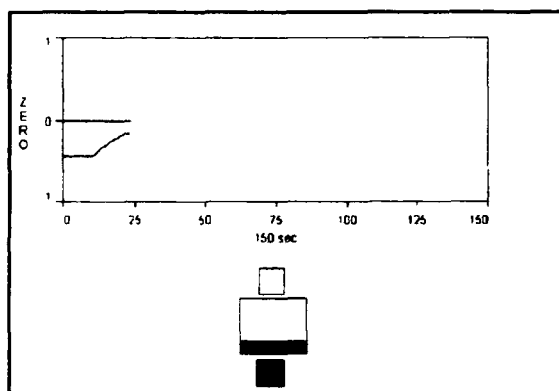


**Figure 22.** ZERO Showing Signal Somewhere Less Than Zero Volts

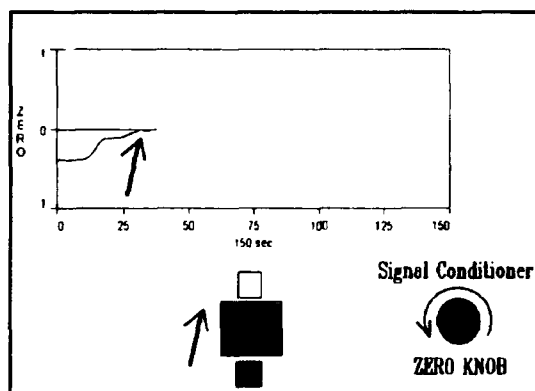


**Figure 23.** ZERO Showing Signal After Being "Flown" Up to Zero Volts

Here are the steps:

1. Using the 486 PC on the right, RECALL ZERO in LabTech Notebook Build-Time.
2. Ensure the tunnel is *not running* by verifying the tunnel water micromanometer does in fact read 0.00 cm with the bottom of the water meniscus just resting on the cross-hair. Verify at the micromanometer, not the PC.
3. Select RUN.
4. The technician has already pre-configured the signal conditioners to yield a ballpark zero. Using the display presented, unlock and turn each "zero" knob on the upper

signal conditioners (#1, 2 and 10) until the colored "meatball" is centered. This is very easy for Naval aviators! A line display reflects the actual zero line for each device. Because of the complexity, the technician will ensure the rotator and traverse are properly scaled.

5. To illustrate the effect of undesired noise on a data acquisition system, turn the DVM on and plug the red probe into the green outlet of the second signal conditioner; plug the black probe into the white outlet. Wait for 30 seconds. What happens to your display? (Don't forget to unplug the DVM probes!)

- 
6. Exit ZERO and repeat step 1 for SPAN.
  7. After the operation brief and safety check of wind tunnel, run the tunnel up to 15 cm H<sub>2</sub>O.
  8. Select RUN. This time, the signal will be referenced to 1.0 (unity).
  9. Again, the technician has already pre-configured the signal conditioners to give ballpark voltage output which, when scaled by the set-ups in LabTech Notebook, will yield 1.0. Using the display presented, unlock and turn each "span" knob on the upper signal conditioners (#1, 2 and 10) until the colored "meatball" is again centered. Another line display reflects the actual 1.0 line for each device. Again, the technician only will ensure the rotator and traverse are properly scaled.
  10. Press "REV" on the rotator control box to reset the cylinder to  $\theta = -20^\circ$ .
  11. The setups are now properly scaled. Leave the tunnel running and proceed to step 1 of the cylinder lab.

## Lab Procedures

### RUN #1

1. RECALL PRE\_DIS1
2. Single-click the "Run" menu and single-click "Run"  
(you will see a window which asks you if you want to "Overwrite previous log(s)?")
3. Single-click "Yes" and expand the window (the display configured for this third of the lab is now present - data acquisition has been "triggered" to begin when the input from the azimuth block passes through  $-17^\circ$  for the first time)
4. Momentarily push the black "FWD" button on the rotator control box, observe the following:
  - a. the cylinder rotates from  $-20$  to  $+180$  degrees
  - b. as the cylinder passes  $-17$  degrees, data is displayed on the PC:  
Azimuth and current time displayed in meter boxes  
X-Y plot showing

Green line: theoretical  $C_p$  vs.  $\theta$

Cyan line: actual raw  $C_p$  vs.  $\theta$  (collected at Sampling Rate of 10 Hz)

Black line: actual smoothed  $C_p$  vs.  $\theta$  (moving average with parameter of 10 points)

- c. boundary layer separation occurs (the wake begins)
  - d. data acquisition stops as cylinder passes through +180 degrees but the display remains on
5. To make a print-out of the display hit ALT-Print Screen (this sends a BitMap to the ClipBoard in Windows)
  6. Single-click "File" then single-click "Exit" to leave the display and return to ICONview (you will be asked "Do you really want to exit?" - single-click "OK")
  7. Exit ICONview by single-clicking "File," "Exit," and "OK" in succession
  8. Double-click "paintbrush" in the Windows Accessories menu
  9. Single-click "View," then deselect (by single-clicking) "Tools and Linesize," and "Palette"
  10. Click the uppermost right button to stretch the paintbrush window to its limits
  11. Select "Edit" and "Paste" (a copy of the previous display will appear)
  12. Select "File" and "Print"
  13. Reduce the scaling to 80% and hit "enter" (the printer will now print a copy of the display)
  14. Select the uppermost "File" and "Exit" (paintbrush will ask you if "you want to save current changes?" - single-click "No")

## **RUN #2**

15. Repeat steps 1,2 substituting WAKE\_AN1 for the first set-up
16. Single-click "Yes" and expand the window (the display configured for this third of the lab is now present - data acquisition has been "triggered" to begin when ALT-1 is pressed on the keyboard...press ALT-1 when the next step is started)
17. Have someone begin cranking the traverse handle at a quick, even, steady rate and observe the following:
  - a. the traverse moves from 0 to 20 inches
  - b. after ALT-1 is pressed, data begin to be displayed on the PC:  
Position and time are displayed in meter boxes

### X-Y plot showing

Blue line: smoothed

$$\left[ \sqrt{\frac{q_w}{q_\infty}} - \frac{q_w}{q_\infty} \right] \text{ vs. } y$$

(moving average with parameter of 25 points and collected at Sampling Rate of 10 Hz)

- c. the position and relative strength of the wake
  - d. data acquisition continues as traverse passes through 19 inches and display remains on
18. Press ALT-Print Screen to save display, then select File and Exit immediately to stop data acquisition. To make a print-out of the display repeat steps 5-14
  19. Stop the wind tunnel at this time using tunnel operating procedures, open test section

### **RUN #3**

20. Repeat ZERO to recalibrate your signals, if necessary.
21. Apply two 1/2" x 20" x 1 mil (approx.) pieces of cellophane tape to cylinder 1 1/4 inches on either side of the static port (this will trip the boundary layer, creating turbulence and thus delaying boundary layer separation)
22. Crank the traverse back to  $y = 0$  and close up the test section
23. Run the tunnel up to 15 cm H<sub>2</sub>O again
24. Repeat SPAN to recalibrate your signals, if necessary.
25. Repeat steps 15-19 substituting WAKE\_AN2 for the second setup (notice that the wake size is reduced)
26. Note the tunnel temperature at shut down:  $T =$  \_\_\_\_\_
27. You are complete - Exit LabTech Notebook and double-click "Exit Windows";
28. Place a formatted disk in either floppy drive. If you are using a 3 1/2" disk, at the DOS prompt type (otherwise substitute A for B):
  - C:\> copy C:\windtunl\pre\_dis1.m B:\pre\_dis1.m (ENTER)
  - C:\> copy C:\windtunl\wake\_an1.m B:\wake\_an1.m (ENTER)
  - C:\> copy C:\windtunl\wake\_an2.m B:\wake\_an2.m (ENTER)This will copy the three data files onto your disk for later analysis.
29. Secure the CPU, Monitor and Printer; ensure the wind tunnel is properly secured.

### **Report Requirements**

1. Using a data analysis program such as MATLAB<sup>®</sup> and data from the lab, calculate the integrals of equations (1) and (2). Be sure to apply proper wake and solid blockage correction factors to find experimental drag coefficients for each of the three runs. See pages 35-38 of the NPS Laboratory Manual for Low Speed Wind

Tunnel Testing for more information. Explain in detail how you found the drag coefficients. List any equations used and how you used them.

2. Using the  $c_{du}$  from Run #1, calculate the effective Reynolds number ( $Re_{EFF}$ ) and determine the corresponding empirical drag coefficient using Figure 24 (from Anderson's Fundamentals of Aerodynamics, p. 229) and

$$Re_{EFF} = Re_{uncorrected}(1 + \epsilon) \cdot TF \quad (8)$$

3. Briefly discuss the differences between the pressure distribution results, the wake analysis results and the empirical drag coefficient.
4. Determine the percentage reduction in drag afforded by an induced turbulent boundary layer. List at least two real-life examples of how turbulence is used to delay the onset of drag (boundary-layer separation).

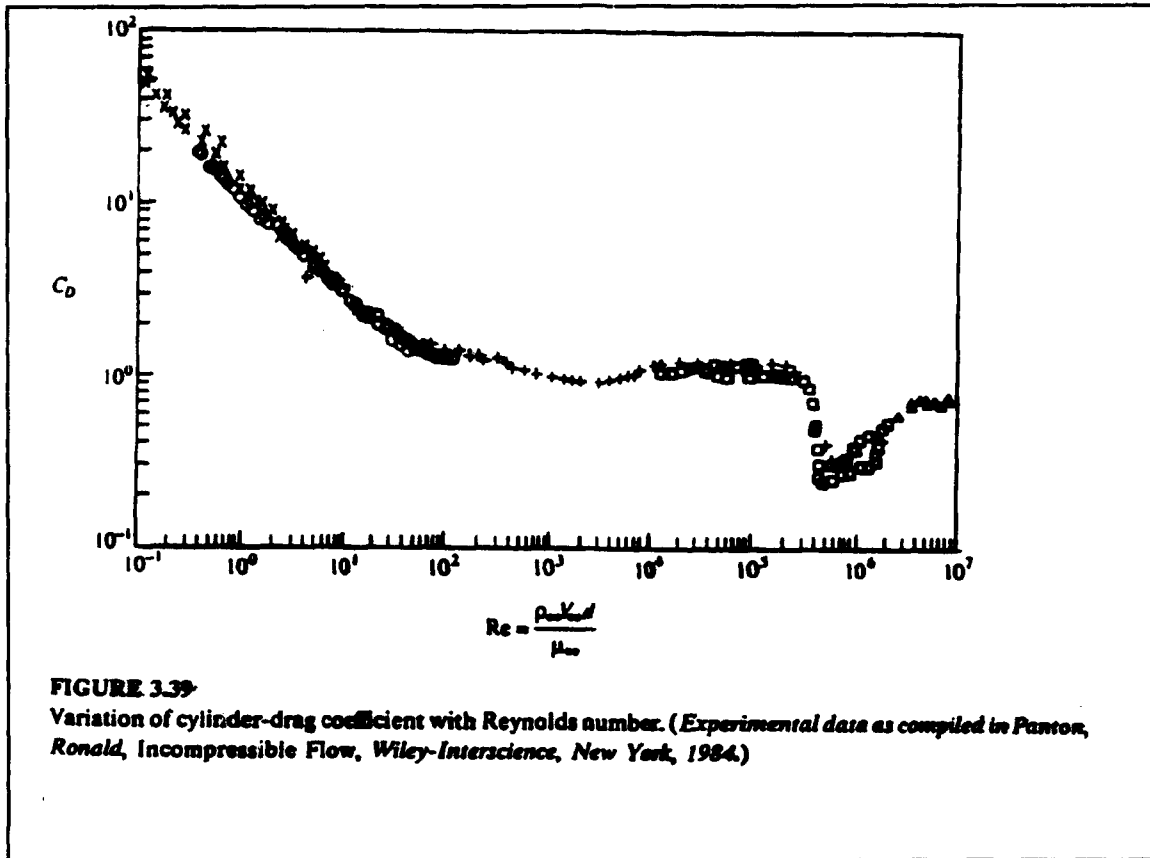


Figure 24. Cylinder Drag Coefficient

# APPENDIX C: UPGRADED LAB DATA

Filename: PRE\_DIS1.m

0.49  
0.48  
0.47  
0.46  
0.45  
0.44  
0.43  
0.42  
0.41  
0.40  
0.39  
0.38  
0.37  
0.36  
0.35  
0.34  
0.33  
0.32  
0.31  
0.30  
0.29  
0.28  
0.27  
0.26  
0.25  
0.24  
0.23  
0.22  
0.21  
0.20  
0.19  
0.18  
0.17  
0.16  
0.15  
0.14  
0.13  
0.12  
0.11  
0.10  
0.09  
0.08  
0.07  
0.06  
0.05  
0.04  
0.03  
0.02  
0.01  
0.00

0.49  
0.48  
0.47  
0.46  
0.45  
0.44  
0.43  
0.42  
0.41  
0.40  
0.39  
0.38  
0.37  
0.36  
0.35  
0.34  
0.33  
0.32  
0.31  
0.30  
0.29  
0.28  
0.27  
0.26  
0.25  
0.24  
0.23  
0.22  
0.21  
0.20  
0.19  
0.18  
0.17  
0.16  
0.15  
0.14  
0.13  
0.12  
0.11  
0.10  
0.09  
0.08  
0.07  
0.06  
0.05  
0.04  
0.03  
0.02  
0.01  
0.00

0.49  
0.48  
0.47  
0.46  
0.45  
0.44  
0.43  
0.42  
0.41  
0.40  
0.39  
0.38  
0.37  
0.36  
0.35  
0.34  
0.33  
0.32  
0.31  
0.30  
0.29  
0.28  
0.27  
0.26  
0.25  
0.24  
0.23  
0.22  
0.21  
0.20  
0.19  
0.18  
0.17  
0.16  
0.15  
0.14  
0.13  
0.12  
0.11  
0.10  
0.09  
0.08  
0.07  
0.06  
0.05  
0.04  
0.03  
0.02  
0.01  
0.00

0.49  
0.48  
0.47  
0.46  
0.45  
0.44  
0.43  
0.42  
0.41  
0.40  
0.39  
0.38  
0.37  
0.36  
0.35  
0.34  
0.33  
0.32  
0.31  
0.30  
0.29  
0.28  
0.27  
0.26  
0.25  
0.24  
0.23  
0.22  
0.21  
0.20  
0.19  
0.18  
0.17  
0.16  
0.15  
0.14  
0.13  
0.12  
0.11  
0.10  
0.09  
0.08  
0.07  
0.06  
0.05  
0.04  
0.03  
0.02  
0.01  
0.00

0.49  
0.48  
0.47  
0.46  
0.45  
0.44  
0.43  
0.42  
0.41  
0.40  
0.39  
0.38  
0.37  
0.36  
0.35  
0.34  
0.33  
0.32  
0.31  
0.30  
0.29  
0.28  
0.27  
0.26  
0.25  
0.24  
0.23  
0.22  
0.21  
0.20  
0.19  
0.18  
0.17  
0.16  
0.15  
0.14  
0.13  
0.12  
0.11  
0.10  
0.09  
0.08  
0.07  
0.06  
0.05  
0.04  
0.03  
0.02  
0.01  
0.00

0.49  
0.48  
0.47  
0.46  
0.45  
0.44  
0.43  
0.42  
0.41  
0.40  
0.39  
0.38  
0.37  
0.36  
0.35  
0.34  
0.33  
0.32  
0.31  
0.30  
0.29  
0.28  
0.27  
0.26  
0.25  
0.24  
0.23  
0.22  
0.21  
0.20  
0.19  
0.18  
0.17  
0.16  
0.15  
0.14  
0.13  
0.12  
0.11  
0.10  
0.09  
0.08  
0.07  
0.06  
0.05  
0.04  
0.03  
0.02  
0.01  
0.00

174.68  
175.18  
175.68  
176.18  
176.68

0.34  
0.33  
0.32  
0.31  
0.30

0.97  
0.96  
0.95  
0.94  
0.93



[illegible]

17	17
20	20
22	22
23	23
24	24
25	25
26	26
28	28
30	30
31	31
32	32
33	33
34	34
35	35
36	36
37	37
38	38
39	39
40	40
41	41
42	42
43	43
44	44
45	45
46	46
47	47
48	48
49	49
50	50
51	51
52	52
53	53
54	54
55	55
56	56
57	57
58	58
59	59
60	60
61	61
62	62
63	63
64	64
65	65
66	66
67	67
68	68
69	69
70	70
71	71
72	72
73	73
74	74
75	75
76	76
77	77
78	78
79	79
80	80
81	81
82	82
83	83
84	84
85	85
86	86
87	87
88	88
89	89
90	90
91	91
92	92
93	93
94	94
95	95
96	96
97	97
98	98
99	99
100	100

[illegible][illegible]

This image displays a highly magnified, vertical view of a material surface. It features a dense, repeating pattern of small, dark, circular or oval shapes, which appear to be part of a larger, textured structure. The pattern is consistent across the entire length of the image, suggesting a uniform material composition or a specific manufacturing process. The overall appearance is that of a microscopic view of a material, possibly a polymer or a metal surface, showing a regular, grid-like arrangement of these small features.









[illegible][illegible][illegible]







## APPENDIX D: MATLAB CODE FOR RETRIEVAL/DATA ANALYSIS

Filename: DRAG1.m

```
% DRAG1.M needs 3 files on a 3-1/2" disk labeled:
% B:\pre_dis1.m; B:\wake_an1.m; B:\wake_an2.m
% If you haven't placed a disk in the B-drive with these three files, as
% named, do so at this time. If you have your files on a 5-1/4" disk,
% you will need to get into this program "DRAG1.m" and edit the lines
% with the load commands to read A vice B, for A-drive.
% Remember, the student version of MATLAB will not execute a file with
% more than 1024 elements. The Wake An files have at least that many.
% Next, it loads these three files into MATLAB and then begins to
% break them down into column vectors for use in a modified Trapezoidal
% rule. Instead of having equispaced x points, as required by the
% trapezoidal rule, the difference between each successive set of x-values
% are multiplied by the average between each associated set of y-values.
% These products are then summed. All cd's are then corrected for blockage.
% The following abbreviations are used:
% cdpdu == uncorrected cd using eqn 2 (for use in Re(eff) calculation)
% Reeff == effective Reynolds number for use w/ Anderson's Figure 3.39
% cdpd1 == cd from pressure distribution method; eqn 1 - equispaced assumed
% cdpd2 == cd from pressure distribution method; eqn 2 - modified trap. mthd.
% pft1 == a polyfit of RUN #1 values was done and a eqn 1 was applied
% cdwa1 == drag coefficient (RUN #2) via the wake analysis method; eqn 2
% cdwa2 == drag coefficient (RUN #3) via the wake analysis method; eqn 2
% sepaz == the azimuth in degrees where separation occurs (estimate)
% wakebeg == the estimated beginning of the wake (in y)
% wakeend == the estimated ending of the wake (in y)
% percrcdu == the % drag reduction afforded by tripping the boundary layer
% Expect some plots after the program finds each cd. Hit any key to continue
% after the computer pauses with each plot or cd. At this time type:
% drag1 after the >> prompt. Watch the B-drive light to
% clue you as to the proximity to your first value. It takes about 73 seconds.
load B:\pre_dis1.m
load B:\wake_an1.m
load B:\wake_an2.m
[m1,n1]=size(pre_dis1);
[m2,n2]=size(wake_an1);
[m3,n3]=size(wake_an2);
x1=pre_dis1(1:m1,1);
y1=pre_dis1(1:m1,2);
x2=wake_an1(1:m2,1);
y2=wake_an1(1:m2,2);
x3=wake_an2(1:m3,1);
y3=wake_an2(1:m3,2);
xx1=x1.*pi/180; % degree* to radian conversion
yy1=y1.*cos(xx1); % each elemental Cp is multiplied by its associated
% cos(theta)
% approx. equispace by letting delta x = total length/# samples; then
% use trapezoidal rule (Holman, eqn. 5-16, p. 193); I call this "eqn. 1":
cdpd1=((y1(m1)-y1(1))/2+(sum(y1)-(y1(m1))))*(xx1(m1)/(m1-1));
% this is only slightly different from eqn. 1; here I do not rely on
% equispaced x-values; instead I sum each successive product of dx and dy;
% I call this "eqn. 2":
for k=2:m1;
    s0(k)=(y1(k-1)+y1(k))/2*abs(xx1(k)-xx1(k-1));
end
cdpd2=sum(s0);
p1=polyfit(xx1,yy1,5); % this makes a polyfit of the values given to a 5th
% degree (order) polynomial
f=polyval(p1,xx1); % this evaluates that polynomial at each x-value
pft1=((f(m1)-f(1))/2+(sum(f)-(f(m1))))*(xx1(m1)/(m1-1)); % eqn 1
for i=2:m2;
    s1(i)=(y2(i-1)+y2(i))/2*abs(x2(i)-x2(i-1)); % eqn 2
end
cdwa1=sum(s1)*2/2.96;
for j=2:m3;
    s2(j)=(y3(j-1)+y3(j))/2*abs(x3(j)-x3(j-1)); % eqn 2
end
cdwa2=sum(s2)*2/2.96;
cdpdu=cdpd2;
Reeff=270477.9*1.04*(1+(.00234+.0329*cdpdu));
Reeff
% this next calculation adds the wake and solid blockage factors
```

```

cdpd1 = cdpd1*(1-3*((0.52*195.43)/(8.8*144)^1.5)-2*((2.96*cdpd1)/(2^45)));
cdpd1
cdpd2 = cdpd2*(1-3*((0.52*195.43)/(8.8*144)^1.5)-2*((2.96*cdpd2)/(2^45)));
cdpd2
pft1 = pft1*(1-3*((0.52*195.43)/(8.8*144)^1.5)-2*((2.96*pft1)/(2^45)));
pft1
pause
plot(xx1,yy1,xx1,f,grid,title('Cp*cos(theta) vs theta'),xlabel('theta'),gtext('5th order polynomial'))
pause
cdwal = cdwal*(1-3*((0.52*195.43)/(8.8*144)^1.5)-2*((2.96*cdwal)/(2^45)));
cdwal
% what is the azimuth (location) where separation occurs?
for t=1:m1;
    if y1(t+3) > y1(t);
        sep = xx1(t);break,end
end
yp = 2*2.96*sin(sep);
sepaz = sep*180/pi;
sepaz
plot(x1,y1,sepaz,y1(t),'o'),grid,title('Cp vs theta'),xlabel('theta'),gtext('separation')
pause
wakebeg = 10-(yp/2);
wakebeg
wakeend = 10+(yp/2);
wakeend
pause
plot(x2,y2),grid,title('q ratios diff vs y'),xlabel('y')
pause
cdwa2 = cdwa2*(1-3*((0.52*195.43)/(8.8*144)^1.5)-2*((2.96*cdwa2)/(2^45)));
cdwa2
percrodu = 100-(cdwa2/cdwal)*100;
percrodu
pause
plot(x3,y3,x2,y2),grid,title('a comparison'),xlabel('y'),gtext('Tripped Boundary Layer')
pause
end

```

## APPENDIX E: MATLAB CODES FOR TUNNEL VELOCITY TABLES

Filename: SPEEDS.m

```
% This Matlab file SPEEDS.m creates conversion columns in different
% units for the NPS Low Speed Wind Tunnel; the equations herein
% are based on data obtained during calibrations made by Professor
% R. Howard and LCDR Clay Miller on 26 April 1993.
%
% This program is written out to show conversions in approximately
% 1 page formats and will pause and wait for any keystroke
% between displays to allow user to print data
%
% You will need to remember the following order of columns:
%
% DEL_P ft/sec m/s kts mph km/hr
%
i = 15:05:1.0; % This is the ref.: cm of H2O on the micromanometer
% in ft/sec:
f = sqrt((2*(i.*(62.35/30.5)-.24326))/(0.89467*.002378));
% in m/s:
m = sqrt((2*(i.*(62.35/30.5)-.24326))/(0.89467*.002378)).3048;
% in kts:
k = sqrt((2*(i.*(62.35/30.5)-.24326))/(0.89467*.002378)).5921;
% in mph:
mi = sqrt((2*(i.*(62.35/30.5)-.24326))/(0.89467*.002378)).6818;
% in km/hr:
km = sqrt((2*(i.*(62.35/30.5)-.24326))/(0.89467*.002378)).1.097;
s = [i' f' m' k' mi' km'];
pause
plot(i,f,grid,xlabel('H2O cm'),ylabel('ft/sec'),title('velocity'))
pause
plot(i,m,grid,xlabel('H2O cm'),ylabel('m/s'),title('velocity'))
pause
plot(i,k,grid,xlabel('H2O cm'),ylabel('kts'),title('velocity'))
pause
plot(i,mi,grid,xlabel('H2O cm'),ylabel('mph'),title('velocity'))
pause
plot(i,km,grid,xlabel('H2O cm'),ylabel('km/hr'),title('velocity'))
pause
end
%
i = 1.0:5:10.0; % This is the ref.: cm of H2O on the micromanometer
% in ft/sec:
f = sqrt((2*(i.*(62.35/30.5)-.24326))/(0.89467*.002378));
% in m/s:
m = sqrt((2*(i.*(62.35/30.5)-.24326))/(0.89467*.002378)).3048;
% in kts:
k = sqrt((2*(i.*(62.35/30.5)-.24326))/(0.89467*.002378)).5921;
% in mph:
mi = sqrt((2*(i.*(62.35/30.5)-.24326))/(0.89467*.002378)).6818;
% in km/hr:
km = sqrt((2*(i.*(62.35/30.5)-.24326))/(0.89467*.002378)).1.097;
s = [i' f' m' k' mi' km'];
pause
plot(i,f,grid,xlabel('H2O cm'),ylabel('ft/sec'),title('velocity'))
pause
plot(i,m,grid,xlabel('H2O cm'),ylabel('m/s'),title('velocity'))
pause
plot(i,k,grid,xlabel('H2O cm'),ylabel('kts'),title('velocity'))
pause
plot(i,mi,grid,xlabel('H2O cm'),ylabel('mph'),title('velocity'))
pause
plot(i,km,grid,xlabel('H2O cm'),ylabel('km/hr'),title('velocity'))
pause
end
%
i = 10.0:5:20.0; % This is the ref.: cm of H2O on the micromanometer
% in ft/sec:
f = sqrt((2*(i.*(62.35/30.5)-.24326))/(0.89467*.002378));
% in m/s:
m = sqrt((2*(i.*(62.35/30.5)-.24326))/(0.89467*.002378)).3048;
% in kts:
k = sqrt((2*(i.*(62.35/30.5)-.24326))/(0.89467*.002378)).5921;
% in mph:
```

```

mi = sqrt((2*(i.*(62.35/30.5)-.24326))/(0.89467*.002378))* .6818;
% in km/hr:
km = sqrt((2*(i.*(62.35/30.5)-.24326))/(0.89467*.002378))*1.097;
s = [i' f' m' k' mi' km']
pause
plot(i,f),grid,xlabel('H2O cm'),ylabel('ft/sec'),title('velocity')
pause
plot(i,m),grid,xlabel('H2O cm'),ylabel('m/s'),title('velocity')
pause
plot(i,k),grid,xlabel('H2O cm'),ylabel('kts'),title('velocity')
pause
plot(i,mi),grid,xlabel('H2O cm'),ylabel('mph'),title('velocity')
pause
plot(i,km),grid,xlabel('H2O cm'),ylabel('km/hr'),title('velocity')
pause
end
%
i = 20.0:5:30.0; % This is the ref.: cm of H2O on the micromanometer
% in ft/sec:
f = sqrt((2*(i.*(62.35/30.5)-.24326))/(0.89467*.002378));
% in m/s:
m = sqrt((2*(i.*(62.35/30.5)-.24326))/(0.89467*.002378))* .3048;
% in kts:
k = sqrt((2*(i.*(62.35/30.5)-.24326))/(0.89467*.002378))* .5921;
% in mph:
mi = sqrt((2*(i.*(62.35/30.5)-.24326))/(0.89467*.002378))* .6818;
% in km/hr:
km = sqrt((2*(i.*(62.35/30.5)-.24326))/(0.89467*.002378))*1.097;
s = [i' f' m' k' mi' km']
pause
plot(i,f),grid,xlabel('H2O cm'),ylabel('ft/sec'),title('velocity')
pause
plot(i,m),grid,xlabel('H2O cm'),ylabel('m/s'),title('velocity')
pause
plot(i,k),grid,xlabel('H2O cm'),ylabel('kts'),title('velocity')
pause
plot(i,mi),grid,xlabel('H2O cm'),ylabel('mph'),title('velocity')
pause
plot(i,km),grid,xlabel('H2O cm'),ylabel('km/hr'),title('velocity')
pause
end

```

## Filename: USER\_SPD.m

```
% This Matlab file USER_SPD.m allows a user to provide MATLAB with
% a desired velocity and have MATLAB return a setting for the water
% micromanometer (in cm H2O) to be used with the NPS Low Speed Wind
% Tunnel; the equations herein are based on data obtained during
% calibrations made by Professor R. Howard and LCDR Clay Miller on
% 26 April 1993.
%
%
i=input('MPH? y/n [n]:','s');
if i=='y'
    k=input('Enter speed desired with a decimal point: ');
    DEL_P=((k./6818)^2*(.89467*.002378/2)+.24326)*(30.5/62.35);
    ('You need to set'),DEL_P
    pause
    j=0.5:.5:40.0;
    p=sqrt((2*(j*62.35/30.5-0.24326))/(.895*.002378))*6818;
    plot(j,p,DEL_P,k,'*'),grid,xlabel('H2O cm'),ylabel('MPH'),title('velocity')
    pause
    break,end
elseif i=='n'
    i=input('Ft/sec? y/n [n]:','s');
    if i=='y'
        k=input('Enter speed desired with a decimal point: ');
        DEL_P=((k.^2*(.89467*.002378/2)+.24326)*(30.5/62.35);
        ('You need to set'),DEL_P
        pause
        j=0.5:.5:40.0;
        p=sqrt((2*(j*62.35/30.5-0.24326))/(.895*.002378));
        plot(j,p,DEL_P,k,'*'),grid,xlabel('H2O cm'),ylabel('Ft/sec'),title('velocity')
        pause
        break,end
    elseif i=='n'
        i=input('m/s? y/n [n]:','s');
        if i=='y'
            k=input('Enter speed desired with a decimal point: ');
            DEL_P=((k./3048)^2*(.89467*.002378/2)+.24326)*(30.5/62.35);
            ('You need to set'),DEL_P
            pause
            j=0.5:.5:40.0;
            p=sqrt((2*(j*62.35/30.5-0.24326))/(.895*.002378))*3048;
            plot(j,p,DEL_P,k,'*'),grid,xlabel('H2O cm'),ylabel('m/s'),title('velocity')
            pause
            break,end
        elseif i=='n'
            i=input('kts? y/n [n]:','s');
            if i=='y'
                k=input('Enter speed desired with a decimal point: ');
                DEL_P=((k./5921)^2*(.89467*.002378/2)+.24326)*(30.5/62.35);
                ('You need to set'),DEL_P
                pause
                j=0.5:.5:40.0;
                p=sqrt((2*(j*62.35/30.5-0.24326))/(.895*.002378))*5921;
                plot(j,p,DEL_P,k,'*'),grid,xlabel('H2O cm'),ylabel('kts'),title('velocity')
                pause
                break,end
            elseif i=='n'
                i=input('km/hr? y/n [n]:','s');
                if i=='n'
                    k=input('Enter speed desired with a decimal point: ');
                    DEL_P=((k./1.097)^2*(.89467*.002378/2)+.24326)*(30.5/62.35);
                    ('You need to set'),DEL_P
                    pause
                    j=0.5:.5:40.0;
                    p=sqrt((2*(j*62.35/30.5-0.24326))/(.895*.002378))*1.097;
                    plot(j,p,DEL_P,k,'*'),grid,xlabel('H2O cm'),ylabel('km/hr'),title('velocity')
                    pause
                    break,end
                else i=='n'
                    end
                end
            end
        end
    end
end
```

## LIST OF REFERENCES

1. *NPS Laboratory Manual for Low Speed Wind Tunnel Testing*, Revised August 1989.
2. Anderson, J.D., *FUNDAMENTALS OF AERODYNAMICS*, 2nd ed., McGraw-Hill, Inc., 1991.
3. Bertin, John J. and Smith, Michael L. *Aerodynamics for Engineers*, Prentice-Hall, Inc., Englewood Cliffs, New Jersey, 1979.
4. Rae, William H., Jr. and Pope, Alan, *Low-Speed Wind Tunnel Testing*, John Wiley & Sons, Inc., 1984.
5. Hoerner, S.F., *FLUID DYNAMIC DRAG*, 2nd ed., (published by author), 1965.
6. Zucker, Robert D., *Fundamentals of Gas Dynamics*, Matrix Publishers, Inc., 1977.
7. *AA2801 Laboratory Manual*, Revised January 1990.
8. Holeman, J.P., *Experimental Methods for Engineers*, 5th ed., McGraw-Hill, Inc., 1989.
9. Panton, R.L., *Incompressible Flow*, John Wiley & Sons, 1984.
10. Winn, A.L. and Logan, A., *The MDHC NOTAR™ SYSTEM*, McDonnell Douglas Helicopter Company, MDHC #90-18, 1990.

### INITIAL DISTRIBUTION LIST

- |    |   |   |
|----|---|---|
| 1. | Defense Technical Information Center<br>Cameron Station<br>Alexandria, VA 22304-6145                | 2 |
| 2. | Library, Code 052<br>Naval Postgraduate School<br>Monterey, CA 93943-5002                           | 2 |
| 3. | Professor Daniel J. Collins, Code AA/Co<br>Naval Postgraduate School<br>Monterey, CA 93943-5000     | 1 |
| 4. | Professor Richard M. Howard, Code AA/Ho<br>Naval Postgraduate School<br>Monterey, CA 93943-5000     | 4 |
| 5. | LCDR Joseph W. Sweeney III, USN, Code AA/MI<br>Naval Postgraduate School<br>Monterey, CA 93943-5000 | 3 |
| 6. | Mr. Jack King, Code AA/Ki<br>Naval Postgraduate School<br>Monterey, CA 93943-5000                   | 1 |
| 7. | LCDR Clay Miller, USN<br>OC DIV, USS SARATOGA, CV-60<br>FPO AA 34078                                | 2 |